A NOVEL AND ROBUST SEMI-AUTOMATED BEST FRAME SELECTION METHOD FROM STRAIN VIDEOS

By

Gulam Mahfuz Chowdhury (142412)
Md. Mahedi Hasan (142402)
Asif Ahmed (142417)
Md. Wahid Tousif Rahman (142465)

A Thesis Submitted to the Academic Faculty in Partial Fulfillment of the Requirements for the Degree of

BACHELOR OF SCIENCE IN ELECTRICAL AND ELECTRONIC ENGINEERING

Department of Electrical and Electronic Engineering
Islamic University of Technology (IUT)
Gazipur, Bangladesh

November 2018

A NOVEL AND ROBUST SEMI-AUTOMATED BEST FRAME SELECTION METHOD FROM STRAIN VIDEOS

Approved by:

Md. Taslim Reza

Supervisor and Assistant Professor,
Department of Electrical and Electronic Engineering,
Islamic University of Technology (IUT),
Boardbazar, Gazipur-1704.

Date: ……

Prof. Dr. Md. Ashraful Hoque

Head of the Department,
Department of Electrical and Electronic Engineering,
Islamic University of Technology (IUT),
Boardbazar, Gazipur-1704.

Date: ……

Contents

List of Tables ..... Error! Bookmark not defined.

List of Figures ..... Error! Bookmark not defined.

List of Acronyms ..... Error! Bookmark not defined.

Acknowledgments ..... Error! Bookmark not defined.

Abstract ..... Error! Bookmark not defined.

1 Introduction ..... Error! Bookmark not defined.

1.1 Ultrasound Imaging ..... **Error! Bookmark not defined.**
1.2 Computer-Aided Diagnosis ..... **Error! Bookmark not defined.**
1.3 Lesion Segmentation ..... **Error! Bookmark not defined.**
1.3.1 Histogram Thresholding and Region Growing . ***Error! Bookmark not defined.***
1.3.2 Watershed-Based Methods ..... ***Error! Bookmark not defined.***

2 Background and Motivation ..... Error! Bookmark not defined.

2.1 Motivation: ..... **Error! Bookmark not defined.**
2.1.1 Ultrasound ..... ***Error! Bookmark not defined.***
2.1.2 Use of Ultrasound ..... ***Error! Bookmark not defined.***
2.2 Elastography ..... **Error! Bookmark not defined.**
2.3 Applications of Elastography ..... **Error! Bookmark not defined.**
2.4 Ultrasound elastography ..... **Error! Bookmark not defined.**
2.5 Elastography in Breast Tumor Detection . **Error! Bookmark not defined.**
2.6 Basic Medical Imaging Methods ..... **Error! Bookmark not defined.**
2.6.1 Ultrasound Imaging ..... ***Error! Bookmark not defined.***
2.6.2 X-Ray Imaging ..... ***Error! Bookmark not defined.***
2.6.3 Computer Tomography ..... ***Error! Bookmark not defined.***
2.6.4 Magnetic Resonance Imaging ..... ***Error! Bookmark not defined.***
2.7 Advantage of Using Ultrasound ..... **Error! Bookmark not defined.**

3 Methodology ..... Error! Bookmark not defined.

3.1 Extracting frames from the video ..... **Error! Bookmark not defined.**
3.2 Pre-processing Frames ..... **Error! Bookmark not defined.**
3.3 Applying MPD & GLCM ..... **Error! Bookmark not defined.**
3.3.1 MPD method: ..... ***Error! Bookmark not defined.***
3.3.2 GLCM: ..... ***Error! Bookmark not defined.***
3.4 Creating a video with the best frames: ..... **Error! Bookmark not defined.**

4 Result and Calculation ..... Error! Bookmark not defined.

4.1 Calculations: ..... **Error! Bookmark not defined.**

5 Discussion ..... Error! Bookmark not defined.

5.1 Demerits of Ultrasound ..... **Error! Bookmark not defined.**
5.2 Future Work ..... **Error! Bookmark not defined.**

References ..... Error! Bookmark not defined.

List of Tables

Table 1.1. Summary of Segmentation Methods for BUS Images……8

Table 2.1: Various parameters of breast tissues……14

Table 4.1: error calculation of 9 videos……...36

List of Figures

FIGURE1. 1: A CAD SYSTEM FOR BREAST CANCER 3

FIGURE2. 1: MAMMOGRAM IMAGE TO DETECT A 11
FIGURE2. 2:ELF 3220 AT UW-MADISON 15
FIGURE2. 3: MANUAL COMPRESSION (QUASISTATIC) ELASTOGRAPHY OF INVASIVE DUCTAL CARCINOMA, A BREAST CANCER. 17
FIGURE2. 4: SUPERSONIC SHEAR IMAGING 21
FIGURE2. 5: BREAST CYST 24
FIGURE2. 6: ULTRASOUND PROBE 25
FIGURE2. 7: SETUP OF ULTRASOUND APPLICATION 26
FIGURE2. 8: CT SCAN MACHINE SETUP 27
FIGURE2. 9: MRI MACHINE SETUP 28

FIGURE3. 1: ALGORITHM OF THE METHOD 31
FIGURE3. 2: US IMAGE OF PRE & POST PROCESSING IMAGE 33

FIGURE4. 1: (A)RESULTS FROM MPD (MEAN PIXEL DIFFERENCE) 45

List of Acronyms

BUS	Breast Ultrasound
MPD	Mean Pixel Difference
GLCM	Gray Level Co-occurrence Matrix
MRI	Magnetic Resonance Imaging
CT	Computed Tomography
US	Ultrasound
ARFI	Acoustic Radiation Forced Imaging
CAD	Computer-Aided Design
BIRAD	Breast Imaging Reporting and Data System
ROI	Region of Interest
DCT	Discrete Cosine Transform
SVM	Support Vector Machine
DCIS	Ductal Carcinoma in Situ
MRF	Markov random fields
SWEI	Shear-wave elasticity imaging
SSI	Supersonic shear imaging
MRE	Magnetic resonance elastography
VA	Vibro-acoustography

Acknowledgments

First of all, we would like to thank Almighty ALLAH for giving us the patience, knowledge, and wisdom to carry out this work. Then we would like to express our sincere gratitude to our supervisor **Md. Taslim Reza** for his kind guidance, encouragement, and support. He has been an extraordinarily wonderful advisor, who has always inspired and motivated us by giving his thoughtful suggestions to overcome the challenges and successfully complete this work.

We are very thankful to our parents, brothers, and sisters, they have done so much for us by encouraging, inspiring and helping us in the pursuit of knowledge, our parents have supported us from our very childhood until this point, they deserve the very best of our appreciation, without their support it would never be possible for us to come this far.

Abstract

Breast cancer is the second leading cause of death of women worldwide. Accurate lesion boundary detection is important for breast cancer diagnosis. Since many crucial features for discriminating benign and malignant lesions are based on the contour, shape, and texture of the lesion, an accurate segmentation method is essential for a successful diagnosis. Ultrasound is an effective screening tool and primarily useful for differentiating benign and malignant lesions. However, due to inherent speckle noise and the low contrast of breast ultrasound imaging, automatic lesion segmentation is still a challenging task. This research focuses on developing a novel, effective, and fully automatic lesion segmentation method for breast ultrasound images. By incorporating empirical domain knowledge of breast structure, a region of interest is generated. Then, a novel enhancement algorithm (using a novel phase feature) and a newly developed neutrosophic clustering method is developed to detect the precise lesion boundary. Neutrosophy is a recently introduced branch of philosophy that deals with paradoxes, contradictions, antitheses, and antinomies. When neutrosophy is used to segment images with vague boundaries, its unique ability to deal with uncertainty is brought to bear. In this work, we apply neutrosophy to breast ultrasound image segmentation and propose a new clustering method named neutrosophic *l*-means. We compare the proposed method with traditional fuzzy c-means clustering and three other well-developed segmentation methods for breast ultrasound images, using the same database. Both accuracy and time complexity are analyzed. The proposed method achieves the best accuracy (TP rate is 94.36%, FP rate is 8.08%, and the similarity rate is 87.39%) with a fairly rapid processing speed (about 20 seconds). Sensitivity analysis shows the robustness of the proposed a method as well. Cases with multiple-lesions and severe shadowing effect (shadow areas having similar intensity values of the lesion and tightly connected with the lesion) is not included in this study. Ultrasound is one of the ways of detecting and identifying breast tumor. From the raw US signal (known as RF data), we get the B-mode image, in which the tumor might not be that much visible. For better tumor visibility, we need to form a strain image. From pre and post compressed US image of the breast, we can estimate strain and form a strain video. Each frame of the video does not have good tumor visibility. It is difficult and time consuming for a doctor to accurately detect the shape of the tumor from rapidly changing frames. Selecting the frames where the tumor is comparably more visible will help the

doctor/radiologist to detect the tumor more easily. In this paper, a method of semi-automated best frame selection from a strain video is proposed. The method involves two ways to select the required frames and to show the best output frames in the form of a video. It is based on Mean Pixel Difference (MPD) and contrast as the Image Descriptors.

Chapter 1

Introduction

Breast cancer is the second leading cause of death for women worldwide, and more than 8% of all women will suffer this disease during their lifetime [1]. According to cancer statistics 2010, it is estimated that 209,060 new cases of breast cancer will be diagnosed and approximately 40,230 deaths are expected in the United States alone [2]. Since the causes of breast cancer still remain unknown, early detection is the key to reduce the death rate (40% or more) [3]. The earlier the cancers are detected, the better the treatment that can be provided. Early detection requires an accurate and reliable a diagnosis which should also be able to distinguish between benign and malignant tumors. Further, a good detection approach should produce both a low false positive rate and a false negative rate.

1.1 Ultrasound Imaging: Until recently, the most effective modality for detecting and diagnosing has been mammography [3, 4]. However, there are limitations of mammography in breast cancer detection. Many unnecessary (65–85%) biopsy operations are due to the low specificity of mammography [5]. The unnecessary biopsies not only increase the cost but also make the patients suffer from emotional pressure. Mammography has also proven less effective in detecting breast cancer in adolescent women with dense breasts. In addition, the ionizing radiation of mammography might be harmful to both patients and radiologists. Ultrasound (US) imaging is an important alternative to mammography. Researchers and practitioners are showing an increasing interest in the use of ultrasound images for breast cancer detection [6-8]. Statistics show that more than one out of every four studies.

1.2 Computer-Aided Diagnosis

Since sonography is much more operator-dependent than mammography, reading ultrasound image requires well-trained and experienced radiologists. Further, even well-trained experts may have a high inter-observer variation rate; therefore, computer-aided diagnosis (CAD) is has been investigated to help radiologists in making accurate diagnoses. One advantage of a CAD system is that it can obtain some features, such as computational features and statistical features, which cannot be obtained visually and intuitively by medical doctors. Another advantage is that CAD can minimize the operator-dependent nature inherent in ultrasound imaging [16] and make the diagnosis process reproducible. It should be noted that research into the use of CAD is not done so with an eye toward eliminating doctors or radiologists, rather the goal is to provide doctors and radiologists a second opinion and help them to increase the diagnosis accuracy, reduce biopsy rate, and save them time and effort. Generally, ultrasound CAD systems for breast cancer detection involve four stages

1. Image preprocessing: The task of image preprocessing is to enhance the image and to reduce speckle without destroying the important features of BUS images for diagnosis.
2. Image segmentation: Image segmentation divides the image into non-overlapping regions, and it separates the objects (lesions) from the background. The boundaries of the lesions are delineated for feature extraction.
3. Feature extraction and selection: This step is to find a feature set of breast cancer lesions that can accurately distinguish lesion/non-lesion or benign/malignant. The feature space could be very large and complex, so extracting and selecting the most effective features are very important.
4. Classification: Based on the selected features, the suspicious regions will be classified into different categories, such as benign findings and malignancy. Many machine learning techniques such as linear discriminant analysis (LDA), support vector machine (SVM) and artificial neural network (ANN) have been studied for lesion classification.

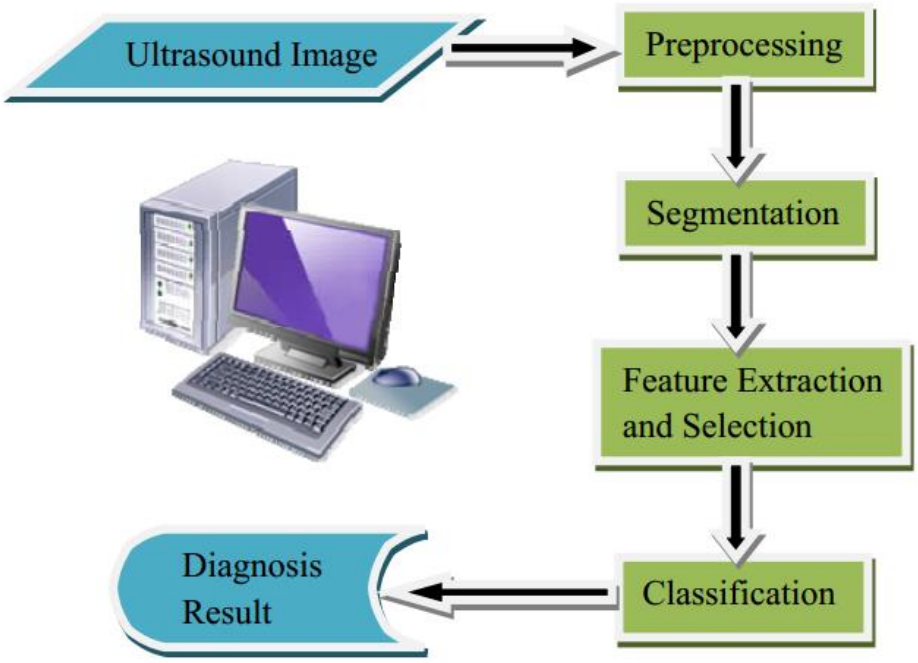

Figure1. 1: A CAD system for breast cancer

1. Image preprocessing: The task of image preprocessing is to enhance the image and to reduce speckle without destroying the important features of BUS images for diagnosis.
2. Image segmentation: Image segmentation divides the image into non-overlapping regions and it separates the objects (lesions) from the background. The boundaries of the lesions are delineated for feature extraction.
3. Feature extraction and selection: This step is to find a feature set of breast cancer lesions that can accurately distinguish lesion/non-lesion or benign/malignant. The feature space could be very large and complex, so extracting and selecting the most effective features are very important.
4. Classification: Based on the selected features, the suspicious regions will be classified into different categories, such as benign findings and malignancy. Many machine learning techniques such as linear discriminant analysis (LDA), support vector machine (SVM) and artificial neural network (ANN) has been studied for lesion classification.

1.3 Lesion Segmentation

Segmentation is an important step in CAD systems. Both automation and accuracy of segmentation is crucial. Automation of segmentation is important because it facilitates the complete automation of the CAD system. A fully automatic CAD can minimize the effect of the operator-dependent nature inherent in ultrasound imaging [16] and make the diagnosis process reproducible. Accuracy of segmentation is important because many crucial features for discriminating benign and malignant lesions are based on the contour, shape, and texture of the lesion (ACR BI-RADS lexicon [17]). These features can be effectively extracted after the lesion boundary is correctly detected. Thus, an accurate segmentation method is essential for a correct diagnosis. However, there are characteristic artifacts, such as attenuation, speckle, shadows, and signal dropout, which make the segmentation task complicated; these artifacts are due to the orientation dependence of acquisition that can result in missing boundaries. Further complications arise as the contrast between areas of interest is often low [18]. How to do one of the oldest image processing tasks, image segmentation, for breast ultrasound, is a challenging task.

Many techniques have been developed for BUS segmentation. They are categorized into histogram thresholding, region growing, model-based (active contour, level set, Markov random field), machine learning, and watershed methods.

1.3.1 Histogram Thresholding and Region Growing

Simple histogram thresholding [19, 20] or region-growing algorithms [21, 22] can find the preliminary lesion boundary. In a histogram thresholding method, an intensity the threshold is chosen at the valley of the image histogram to separate the image into background and foreground. For a region growing method, a region is grown from the seed point (start point) by adding similar neighboring pixels. Although efficient, these methods cannot generate a precise boundary because of their over-simplified concepts and the high sensitivity to noise. However, they can serve as an intermediate step to provide a rough contour [21] or can be combined with post-processing procedures such as morphological operations [19, 20, 23], disk expansion [24], Bayesian neural network [12], function optimization [25, 26], etc. For example, in the thresholding algorithm [19, 20], firstly, the regions of interest (ROIs) were preprocessed with a 4×4 median filter to

reduce the speckle noise and to enhance the features. Second, a 3×3 unsharp filter was constructed using the negative of a two-dimensional Laplacian filter to emphasize the elements with meaningful signal level and to enhance the contrast between object and background. Third, the ROIs were converted to a binary image by thresholding. The the threshold was determined by the histogram of ROIs. If a valley of a histogram between 33% and 66% of the pixel population could be found, this intensity value was selected as the threshold. If there was no such valley in that range, the intensity of 50% of the pixel the population was selected as the threshold value. Finally, the selected nodule's boundary pixels were obtained using morphologic operations.

1.3.2 Model-Based Methods

Model-based methods have strong noise-resistant abilities and are relatively stable at sonography demarcation. Commonly used models include level set [27-29], active contours [21, 30-33], Markov random fields (MRF) [34-38], etc.
For instance, Sarti et al. [29] discussed a level set maximum likelihood method to achieve a maximum likelihood segmentation of the target. The Rayleigh probability distribution was utilized to model the gray level behavior of ultrasound images. A partial the differential equation-based flow was derived as the steepest descent of an energy function considering the density probability distribution of the gray levels, as well as smoothness constraints. A level set formulation for the associated flow was derived to search the minimal value of the model. Finally, the image was segmented according to the minimum energy.

Madabhushi and Metaxas [21] combined intensity, texture information, and empirical domain knowledge used by radiologists with an active contour model in an attempt to limit the effects of shadowing and false positives. Their method requires training but in the small database. Using manual delineation of the mass by a radiologist as a reference, and the Hausdorff distance and average distance as boundary error metrics, they showed that their method is independent of the number of training samples, shows good reproducibility with respect to parameters, and gives a true positive area of 74.7%. Some active contour models have been applied to 3-D ultrasound segmentation, such as [30-33]. Boukerroui et al. [34] used a Markov random field to model the region process and to focus on the adaptive characteristics of the algorithm. Their method introduced a function

to control the adaptive properties of the segmentation process, and took into account both local and global statistics during the segmentation process. A new formulation of the segmentation problem was utilized to control the effective contribution of each statistical component. The merit of MRF modeling is that it provides a strong exploitation of the pixel correlations. The segmentation results can be further enhanced via the application of maximum a posteriori segmentation estimation scheme based on the Bayesian learning paradigm [18].

In most model-based approaches, an energy function is formulated, and the segmentation problem is transformed as finding the minimum (or maximum) of the energy function iteratively. However, the iterations on calculating energy functions and reformulating the models are always time-consuming, especially for complex BUS images; and many models are semi-automatic with the requirement of pre-labeled ROI or manually initialized contour.

1.3.3 Machine Learning Methods

Machine learning methods (such as neural network and support vector machine) [39-43] are popular in image segmentation, which transforms the segmentation problem into a classification decision based on a set of input features. In [42], Dokur and Ölmez proposed a neural network-based segmentation method. Images were divided into square blocks and features were extracted from each block using the discrete cosine transform (DCT). Then a three-layer hybrid neural network was trained to classify the blocks into two categories: background and foreground. The method was applied to the region of interest (ROI) which needed to be selected by the user. Kotropoulos and Pitas [39] employed a support vector machine with a radial basis function kernel to classify different patterns. In this method, patterns were collected by a running window with size of 15x15 over the entire image. To train the SVM, 1128 positive patterns (lesion) and 1128 negative patterns (background) were selected from the training set. Experiments showed that the trained SVM could generate reasonable segmentation result.
For machine learning methods, feature selection and training process are two key steps that play an important role in segmentation result. If features are sufficiently distinguishable and the method is well trained, machine learning methods can generate satisfactory lesion contours. However, over-training or insufficient training (trapped by

local minimum) may severely affect the segmentation performance on new data. And the the training process is usually quite time-consuming.

1.3.4 Watershed-Based Methods

Watershed-based approaches have shown promising performances for ultrasound image segmentation. The methods consider the image as topographic surface wherein the grey level of a pixel is interpreted as its altitude. Water flows along a path to finally reach a local minimum. The biggest challenge for such methods is over-segmentation; to address the problem, many approaches have been proposed and can be categorized into two types: marker-controlled [44-46] and cell competition [47-49]. Marker-controlled methods inundate the gradient landscape of image and define watersheds when the flooding of distinct markers rendezvous with each other. Hence, the identification of makers is very crucial in solving the over-segmentation problem. The the method proposed in [44] was a texture-based approach that selected the marker candidates as seeds for the water-level immersion. A self-organization map was trained to identify the texture of lesions as the flooding markers. Distinctively, the method in [45] adopted a thresholding and morphological operation scheme to seek flooding markers. It required a heuristic estimation of the best thresholding of markers to achieve the task of lesion delineation.

Cell competition approaches, on the other hand, alleviate the over-segmentation the problem in a different way. A two-pass watershed transformation [47] was performed to generate the cell tessellation on the original ultrasound image or ROI. In this method, a competition scheme based on the cell tessellation was carried out by allowing merge and split operations of cells. The cost function was devised to characterize boundary saliency and regional homogeneity of an image partition, and it drove the competition process to converge to a prominent component structure. However, neither marker-controlled nor cell competition approaches guarantee to solve the over-segmentation problem completely [48].

Commonly used segmentation approaches are summarized in Table 1.1. which is given on the next page

Methods	Descriptions	Advantages	Disadvantages
Histogram thresholding	The threshold value is selected to segment the image.	Simple and fast.	Only works for bimodal histograms and has no good results for BUS images
Region growing	The region is grown from the seed point by adding similar neighboring pixels.	The concept is simple. Multiple stop criteria can be chosen.	A seed point is required; sensitive to noise.
Model-based (includes active contour, level set, Markov random fields)	A model is used to formulate the lesion contour and the model is revised based on local features such as edges, intensity gradient, texture, and so on.	Robust, self adapting in search of a minimal energy state.	Time-consuming; pre labeled ROI or initial contour is required; easy to get stuck in local minima states.
Machine learning	Features to separate the lesion from the background are extracted first, and a machine the learning method is trained to do the classification based on pixel-level or region-level.	Stable; different lesion characteristics can be incorporated by feature extraction.	Long training time; over-training problem; test images should come from the same platform as the training images.
Watershed (includes marker-controlled watershed and cell competition watershed)	Considers image as topographic surface wherein grey level of a pixel is interpreted as its altitude. Water flows along a path to finally reach a local minimum.	It ensures closed region boundaries.	Over-segmentation problem is not completely solved.

Table 1.1. Summary of Segmentation Methods for BUS Images.

In summary, the major drawbacks of current methods are:

1) Human interactions such as the pre-labeled ROIs or manually initialized contours are required, which impede full automation;

2) Intensity features are most typically used for boundary detection. Since BUS images have low contrast and are degraded by speckle noise, features based on intensity gradients are always sensitive to noise and cannot guarantee accurate segmentation result;

3) Reformulating the models and training the methods are always time-consuming, especially for complex BUS images. As the image resolution increases, the computational complexity for processing a BUS image also increases.

Chapter 2

Background and Motivation

2.1 Motivation:

Breast Cancer is one of the leading causes of death due to cancer among women all over the world. If it can be detected in the early phase, the chances of curing it become high. Breast cancer originates from a breast tumor. Breast tumors are of two types – Benign and Malignant. The malignant type tumor results in cancer. So, detecting the tumor at an early phase and taking measures to cure it can decrease the chances of producing cancer and thus can save a life.

The existing methods of detecting breast tumor lesion includes Breast Exam, Mammogram, MRI, Biopsy, and Ultrasonography. The details of these methods are given below:

Breast exam: The doctor will check both of the breasts and lymph nodes in the armpit, feeling for any lumps or other abnormalities. Lump, Inverse/ Pulled in nipples, dimpling, dripping, redness/rush, skin change are the symptoms indicating breast tumor. This method can give a vague idea about the existence of tumor lesion inside the breast. But it doesn't give any information about the tumor being benign or malignant. Thus, it cannot be reliably used to identify the condition of the tumor.

Mammogram: Mammography is an imaging technique used for diagnostic screening and surveillance imaging of breast cancer. Using low energy x-rays and standardized views of the breast, mammograms can be used to inspect breast tissues for lumps, lesions, and calcification. Early mammographic examinations can reveal cancer symptoms to the radiologists which allow early treatment and hence increased survival rates(WHO, n.d.). A mammogram is an x-ray picture of the breast. It can also have drawbacks. Mammograms can sometimes find something that looks abnormal but isn't cancer. This leads to further testing and can cause you anxiety. Sometimes mammograms can miss cancer when it is there. [1] Women with dense

breasts have more false-negative results. False-positive results are more common in women who are younger, have dense breasts, have had breast biopsies, have breast cancer in the family, or are taking estrogen. Screening mammograms can find invasive breast cancer and ductal carcinoma in situ (DCIS, cancer cells in the lining of breast ducts) that need to be treated. But it's possible that some of the invasive cancers and DCIS found on mammograms would never grow or spread. (Finding and treating cancers that would never cause problems is called overdiagnosis.) These cancers are not life-threatening and never would have been found or treated if the woman had not gotten a mammogram. The problem is that doctors can't tell these cancers from those that will grow and spread. [2]

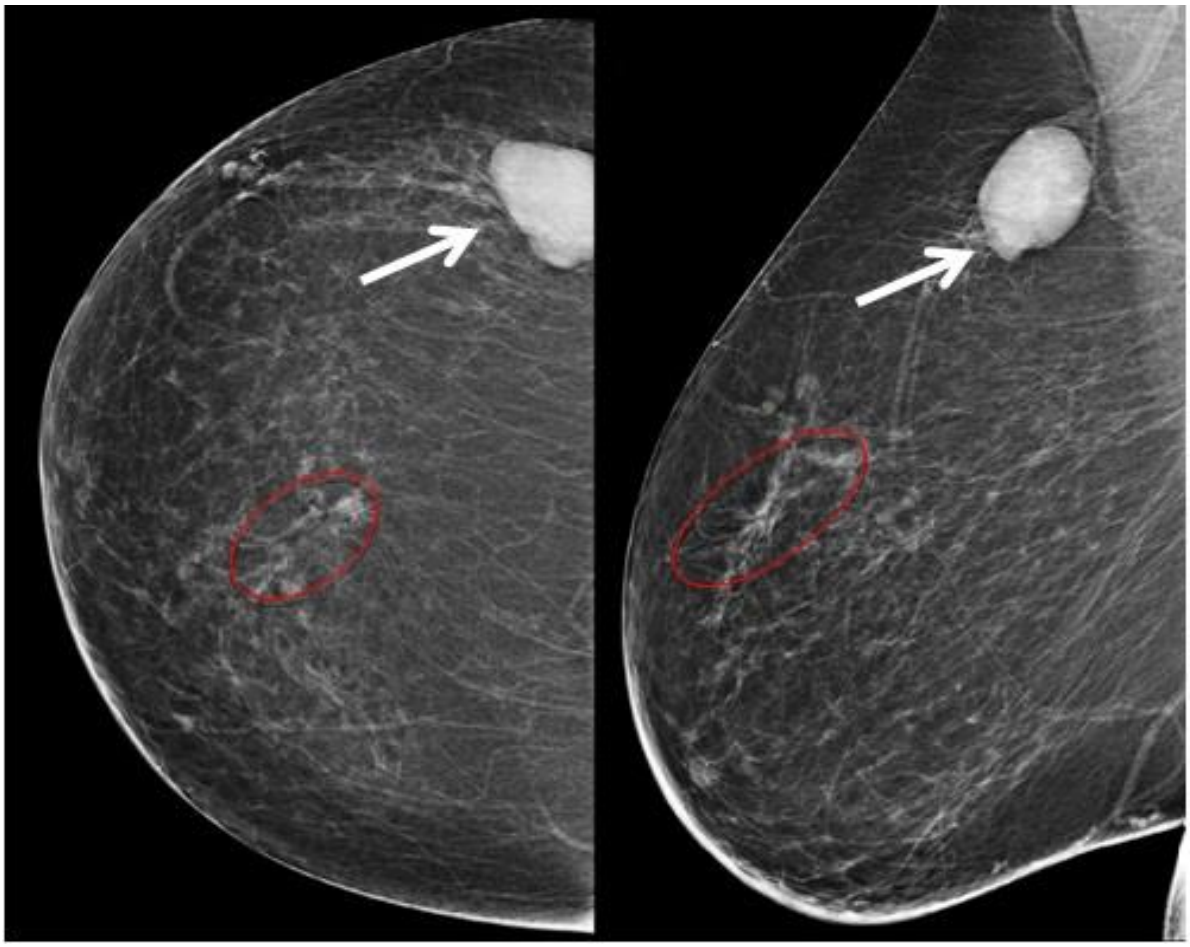

Figure2 1: Mammogram image to detect a

2.1Ultrasound

Ultrasound is sound waves with frequencies higher than the upper audible limit of human hearing. Ultrasound is not different from "normal" (audible) sound in its physical properties, except that humans cannot hear it. This limit varies from person to person and is approximately

20 kilohertz (20,000 hertz) in healthy young adults. Ultrasound devices operate with frequencies from 20 kHz up to several gigahertz.

2.1.1 Use of Ultrasound

Most people associate ultrasound scans with pregnancy and breast imaging. These scans can provide an expectant mother with the first view of her unborn child. However, the test has many other uses like detecting a tumor in the breast.

Some other uses:

- bladder
- brain (in infants)
- eyes
- gallbladder
- kidneys
- liver
- ovaries
- pancreas
- spleen
- thyroid
- testicles
- uterus
- blood vessels

2.2 Elastography

Elastography is a medical imaging modality that maps the elastic properties and stiffness of soft tissue. The main idea is that whether the tissue is hard or soft will give diagnostic information about the presence or status of a disease. For example, cancerous tumors will often be harder than the surrounding tissue, and diseased livers are stiffer than healthy ones.

The most prominent techniques use ultrasound or magnetic resonance imaging (MRI) to make both the stiffness map and an anatomical image for comparison.

Some Definitions:

Stress: Stress is defined as force per unit area.

Shear stress: Shear stress has the same units as normal stress but represents a stress that acts parallel to the surface (cross-section).

Strain: Strain is the change in length per unit length. Computed as *(Lf - L0) / L0* where *Lf* is the final length and *L0* is the initial length.

Strain Rate: Strain Rate specifies how quickly (or slowly) a material is being deformed or loaded, i.e. the amount of strain that occurs in a unit of time. Since strain is dimensionless, units are *1/time*.

Young's Modulus: Young's Modulus is the constant of proportionality between stress and strain. Units are the same as stress (i.e., force per unit area) and the most commonly used are psi, Pa (Pascal), kPa, and MPa.

Poisson's Ratio: Poisson's Ratio is the ratio of lateral strain to longitudinal strain. The typical range of values is between zero and 0.5.

Basic Principles

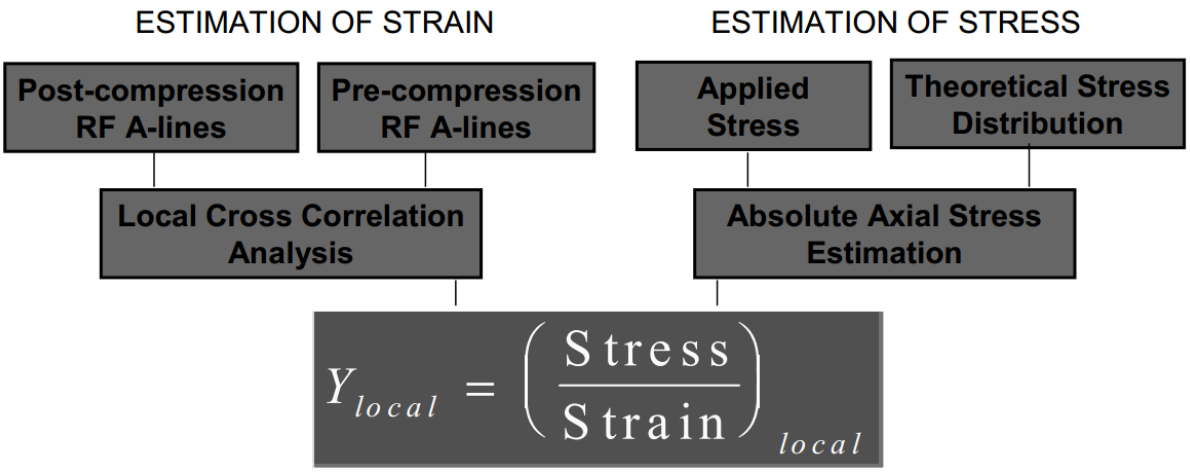

- Tissue Elasticity Imaging methods are based on imaging differences in stiffness or Young's Modulus between normal and abnormal tissue conditions.
- Literature reports on stiffness variations between different tissue types are limited.
- However, these results demonstrate significant stiffness variations between normal and pathological tissue.

Measurements of breast tissues *in-vitro**

Tissue Type	Number Of Patients	Tissue Stiffness (kPa) 20% Pre-compression 20%/sec Strain Rate
Normal Fat	40	20 ± 6
Normal Glandular	31	57 ± 19
Fibrous	21	233 ± 59
Ductal Tumor	23	301 ± 58
Infiltrating Ductal Tumor	32	490 ± 112

**Krouskop TA, Wheeler TM, Kallel F, Garra BS, Hall T., Elastic moduli of breast and prostate tissues under compression, Ultrason Imaging, 1998; 20(4): 260-74.*

Table 2.1: Various parameters of breast tissues

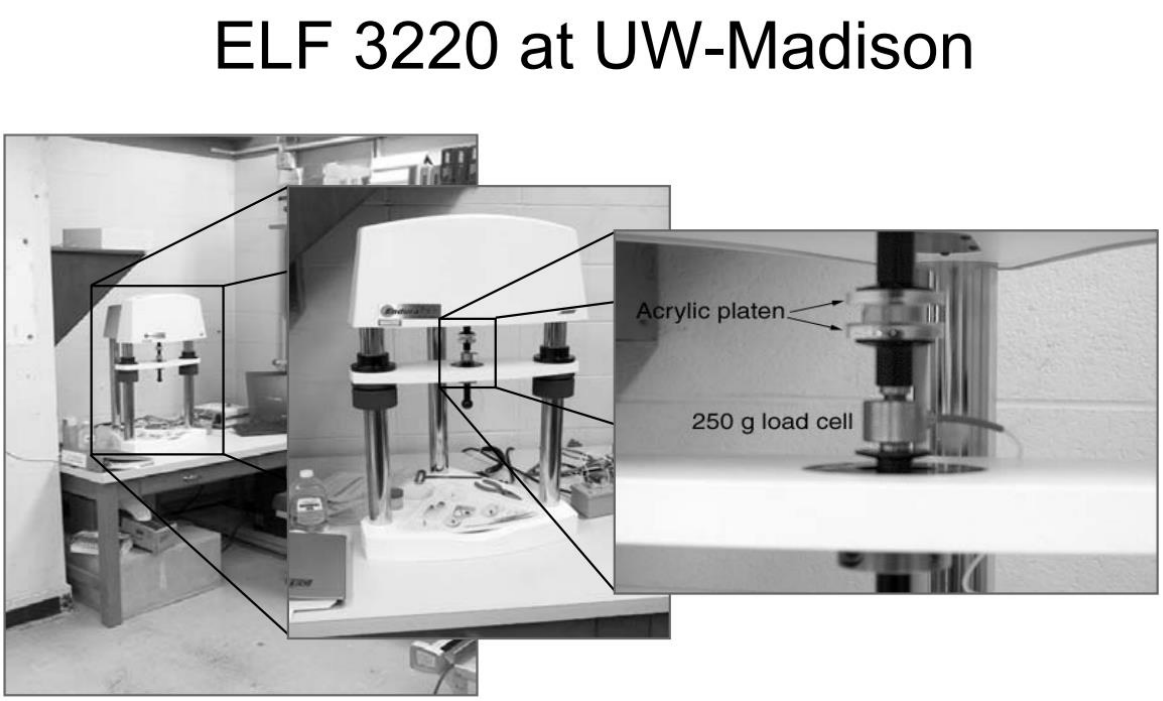

Figure2 2:ELF 3220 at UW-Madison

2.2.1 Applications of Elastography

Elastography is used for the investigation of many disease conditions in many organs. It can be used for additional diagnostic information compared to a mere anatomical image, and it can be used to guide biopsies or, increasingly, replace them entirely. Biopsies are invasive and painful, presenting a risk of hemorrhage or infection, whereas elastography is completely noninvasive.

Elastography is used to investigate disease in the liver. Liver stiffness is usually indicative of fibrosis or steatosis, which are in turn indicative of numerous disease conditions, including cirrhosis and hepatitis. Elastography is particularly advantageous in this case because when fibrosis is diffuse, a biopsy can easily miss sampling the diseased tissue, which results in a false negative misdiagnosis.

Naturally, elastography sees a use for organs and diseases where manual palpation was already widespread. Elastography is used for detection and diagnosis of breast, thyroid and prostate cancers. Certain types of elastography are also suitable for musculoskeletal imaging, and they can determine the mechanical properties and state of muscles and tendons.

Because elastography does not have the same limitations as manual palpation, it is being investigated in some areas for which there is no history of diagnosis with manual palpation. For example, magnetic resonance elastography is capable of assessing the stiffness of the brain, and there is a growing body of scientific literature on elastography in healthy and diseased brains.

Preliminary reports on elastography used on transplanted kidneys to evaluate cortical fibrosis have been published showing promising results.

2.2.2 Ultrasound elastography

There are great many ultrasound elastographic techniques. The most prominent are highlighted below.

Quasistatic elastography/strain imaging

Quasistatic elastography (sometimes called simply 'elastography' for historical reasons) is one of the earliest elastography techniques. In this technique, an external compression is applied to tissue, and the ultrasound images before and after the compression are compared. The areas of the image that are least deformed are the ones that are the stiffest, while the most deformed areas are the least stiff. Generally, what is displayed to the operator is an image of the relative distortions (strains), which is often of clinical utility.

From the relative distortion image, however, making a quantitative stiffness map is often desired. To do this requires that assumptions be made about the nature of the soft tissue being imaged and about tissue outside of the image. Additionally, under compression, objects can move into or out of the image or around in the image, causing problems with interpretation. Another limit of this technique is that like manual palpation, it has difficulty with organs or tissues that are not close to the surface or easily compressed.

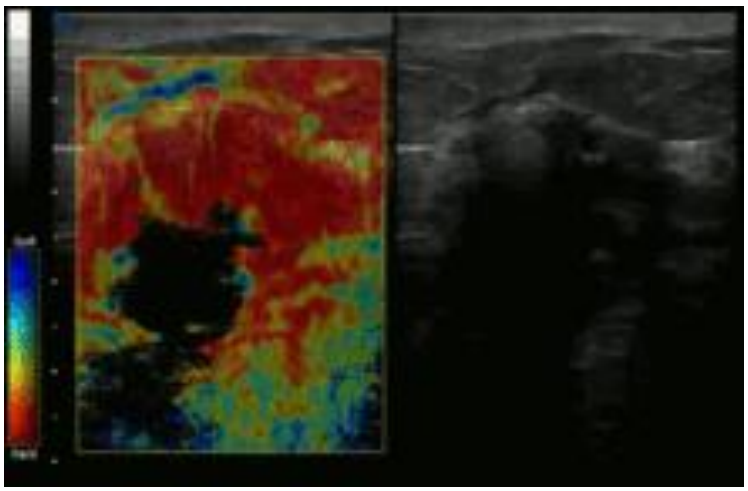

Figure2 3: Manual compression (quasistatic) elastography of invasive ductal carcinoma, a breast cancer.

Acoustic radiation force impulse imaging (ARFI)

One of the major problems in the model-based reconstructive approaches is the need to incorporate boundary conditions to solve the forward problem. In practice, boundary conditions in tissue could be very complicated and the error in the definition of boundary conditions could significantly reduce the quality of reconstruction. A possible solution to

this problem was suggested in where acoustic radiation force of the focused ultrasound wave was used to induce the motion of the tissue. The dynamics of this highly localized motion is defined by the parameters of acoustic excitation and the mechanical properties of tissue, and only weakly depends on the boundary conditions. Analytical equations describing the spatial and temporal behavior of the radiation force induced shear displacement and waves in tissue-like media have been derived in. Figures 3 and 4 adapted from [38] illustrate the calculated tissue response to acoustic radiation force generated by a focused ultrasonic wave.

Figure 3 shows the distribution of axial displacement induced by a focused ultrasonic beam with a 3 MHz carrier frequency modulated with a 1 kHz sinusoid and spatial- and temporal peak intensity of 10 W/cm2. The parameters of tissue were chosen close to those of liver. The spatial distribution of axial displacement at an arbitrarily chosen time is shown. The absolute maximum of the displacement is near the geometric focus on the axis of the ultrasound beam. Neighboring local minima and maxima are about a half wavelength from each other. Figure 3 shows only axial displacement, however, that radial displacement is an order of magnitude smaller than axial displacement .

Figure 4 illustrates the temporal behavior of the axial displacement in the focal plane, i.e., in the plane near the geometric focus of the transducer and parallel to the beam axis. A rectangular 100 μs duration acoustic pulse and a tissue with shear wave speed 5.2 m/s were used in this simulation. Initially, displacement magnitude along the beam axis increases with time. This increase continues due to inertia for some time after the acoustic pulse is terminated. Displacement reaches its maximum at the time needed for the shear wave to travel the distance equal to the depth of the focal region. After reaching the maximum, the displacement starts to decrease, due to the absorption of the shear wave as well as due to the formation of a diverging cylindrical wave propagating away from the axis. At that stage, the the distance between the wavefront and the axis of the beam linearly increases as in accordance with the speed of the shear wave, which is proportional to the square of shear elasticity modulus (in an infinite, isotropic and homogeneous medium).

Local viscoelastic properties of tissue may also be evaluated from the data on tissue motion induced by a radiation force impulse in the focal region of the focused ultrasound beam, which is the basis of Acoustic Radiation Force Impulse (ARFI) imaging.

Here, we consider an example of the model-based reconstructive approach based on a semianalytical solution for focused ultrasound loading. In the case of the tissue response to the focused ultrasound radiation force impulse, the problem is symmetrical with respect to the direction of the ultrasound beam. Therefore, the problem could be considered in a cylindrical coordinate system (r,φ,z), where the z-axis is aligned with the acoustic radiation force F. Displacements and force depend only on coordinates r and z. In cylindrical coordinates the equations of dynamic equilibrium (1) has a form:

$$\frac{\partial \sigma_{rr}}{\partial r}+\frac{\partial \sigma_{rz}}{\partial z}+\frac{(\sigma_{rr}-\sigma_{\varphi\varphi})}{r}=\rho\frac{\partial^2 u_r}{\partial t^2},$$
$$\frac{\partial \sigma_{rz}}{\partial r}+\frac{\partial \sigma_{zz}}{\partial z}+\frac{\sigma_{rz}}{r}+F=\rho\frac{\partial^2 u_z}{\partial t^2},$$

where ur, uz and σrr, σzz, $\sigma\varphi\varphi$, σrz are components of displacement vector and stress tensor in the cylindrical coordinate system. An incompressible medium with zero volume viscosity was assumed in (2). Using the Hankel transform of the force F, displacements ur, uz and the pressure p, equations (12) are reduced to a single differential equation for function W:

$$\frac{\partial^2(\alpha^2 W - W'')}{\partial t^2}+\frac{\mu L(W)}{\rho}+\frac{\mu^*}{\rho}\frac{\partial L(W)}{\partial t}-\frac{\alpha^2 f}{\rho}=0,$$

where $L(W) = WIV - 2\alpha 2W'' + \alpha 4W$, primes mean differentiation with respect to z, W and f are the Hankel transforms of the displacement uz and the force F, respectively, and α is the variable of integration:

$$F(r,z,t)=\int_0^\infty \alpha f(\alpha,z,t)J_0(\alpha r)d\alpha \cdot u_z(r,z,t)=\int_0^\infty \alpha W(\alpha,z,t)J_0(\alpha r)d\alpha$$

The boundary conditions for (13) assume that W and W' are zero away from the focus. If the dependence $f(\alpha,z,t)$ is known or can be evaluated, equation (13) can be solved numerically using, for example, a three-level difference scheme. Thereby, the general 3D problem is reduced to a 1D problem, which can be solved fast and with high accuracy. Figures 5a and 5b present the time dependence of the axial displacement uz at the focal point for various elastic and viscous properties of the medium. In the calculations the load was distributed over the focal spot as an ellipsoid of rotation.

The results show that the time dependence of the displacement is sensitive to changes in the mechanical properties of the medium. An increase in elasticity of the medium leads to the decrease in both displacement magnitude and time needed for the displacement to reach the maximum. High viscosity reduces the displacement amplitude and increases the relaxation time.
Using the solution to this forward problem, the inverse problem can be solved by minimizing the error function

In shear-wave elasticity imaging (SWEI), similar to ARFI, a 'push' is induced deep in the tissue by acoustic radiation force. The disturbance created by this push travels sideways through the tissue as a shear wave. By using an imaging modality like ultrasound or MRI to see how fast the wave gets to different lateral positions, the stiffness of the intervening tissue is inferred. Since the terms "elasticity imaging" and "elastography" are synonyms, the original term SWEI denoting the technology for elasticity mapping using shear waves is often replaced by SWE. The principal difference between SWEI and ARFI is that SWEI is based on the use of shear waves propagating laterally from the beam axis and creating elasticity map by measuring shear wave propagation parameters whereas ARFI gets elasticity information from the axis of the pushing beam and uses multiple pushes to create a 2-D stiffness map. No shear waves are involved in ARFI and no axial elasticity assessment is involved in SWEI. SWEI is implemented in supersonic shear imaging (SSI), one of the most advanced modalities of ultrasound elastography.

Supersonic shear imaging (SSI)

Supersonic shear imaging (SSI) gives a quantitative, real-time two-dimensional map of tissue stiffness. SSI is based on SWEI: it uses acoustic radiation force to induce a 'push' inside the tissue of interest generating shear waves and the tissue's stiffness is computed from how fast the resulting shear wave travels through the tissue. Local tissue velocity maps are obtained with a conventional speckle tracking technique and provide a full movie of the shear wave propagation through the tissue. There are two principal innovations implemented in SSI. First, by using many near-simultaneous pushes, SSI creates a source of shear waves which is moved through the medium at a supersonic speed. Second, the generated shear wave is visualized by using ultrafast imaging technique. Using inversion algorithms, the shear elasticity of medium is mapped quantitatively from the wave propagation movie. SSI is the first ultrasonic imaging

technology able to reach more than 10,000 frames per second of deep-seated organs. SSI provides a set of quantitative and in vivo parameters describing the tissue mechanical properties: Young's modulus, viscosity, anisotropy.

This approach demonstrated clinical benefit in breast, thyroid, liver, prostate and musculoskeletal imaging. SSI is used for breast examination with a number of high-resolution linear transducers. A large multi-center breast imaging study has demonstrated both reproducibility and significant improvement in the classification of breast lesions when shear wave elastography images are added to the interpretation of standard B-mode and Color mode ultrasound images.

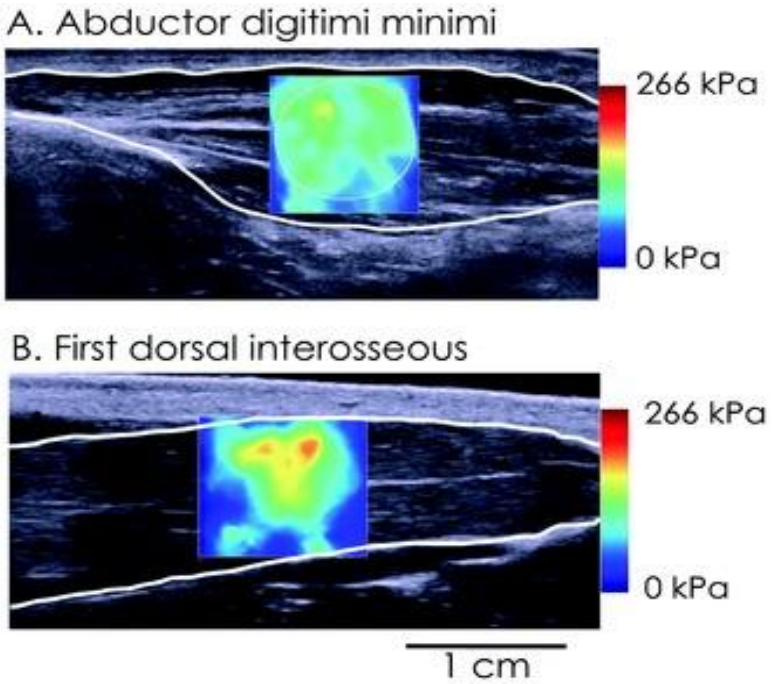

Figure2 4: Supersonic shear imaging

Transient elastography

Transient elastography gives a quantitative one-dimensional (i.e. a line) image of tissue stiffness. It functions by vibrating the skin with a motor to create a passing distortion in the tissue (a shear wave), and imaging the motion of that distortion as it passes deeper into the body using a 1D ultrasound beam. It then displays a quantitative line of tissue stiffness data (Young's modulus). This technique is used mainly by the Fibroscan system, which is used for liver assessment, for example, to diagnose cirrhosis. Because of the prominence of the Fibroscan brand, many clinicians simply refer to transient elastography as 'Fibroscan'.

Magnetic resonance elastography (MRE)

Magnetic resonance elastography (MRE) was introduced in the mid-1990s, and multiple clinical applications have been investigated. In MRE, a mechanical vibrator is used on the surface of the patient's body; this creates shear waves that travel into the patient's deeper tissues. An imaging acquisition sequence that measures the velocity of the waves is used, and this is used to infer the tissue's stiffness (the shear modulus). The result of an MRE scan is a quantitative 3-D map of the tissue stiffness, as well as a conventional 3-D MRI image.

One strength of MRE is the resulting 3D elasticity map, which can cover an entire organ. Because MRI is not limited by air or bone, it can access some tissues ultrasound cannot, notably the brain. It also has the advantage of being more uniform across operators and less dependent on operator skill than most methods of ultrasound elastography.

MR elastography has made significant advances over the past few years with acquisition times down to a minute or less and has been used in a variety of medical applications including cardiology research on living human hearts. MR elastography's short acquisition time also make it competitive with other elastography techniques.

Vibro-acoustography (VA)

Vibro-acoustography (VA) is a method that uses the acoustic response (acoustic emission) of an object to the harmonic radiation force of ultrasound for imaging and material characterization. The acoustic emission is generated by focusing two ultrasound beams of slightly different frequencies at the same spatial location and vibrating the tissue as a result of ultrasound radiation force exerted on the object at a frequency equal to the difference between the frequencies of the primary ultrasound beams. The two focused ultrasound beams of slightly different frequencies $f1$ and $f2$ ($\Delta f = f1\text{-}f2 \ll f1, f2$) intersect at their joint focal point. For typical vibro-acoustography applications, $f1$ and $f2$ are on the order of 2–5 MHz and Δf is typically 10–70 kHz such that there are at least two orders of magnitude in difference ensuring that $\Delta f = \ll f1, f2$. The radiation force from these two beams has a component at Δf (called dynamic ultrasound radiation force), which vibrates the object. The acoustic response of the object to this force is detected by a hydrophone. The co-focus of the ultrasound beams is raster scanned across the object, and the resulting acoustic signal is recorded. An image of the object is formed

by modulating the brightness of each image pixel proportional to the amplitude of the acoustic signal from the excitation point of the object.

Vibro-acoustography images have some unique characteristics that set it apart from traditional ultrasound imaging. This is partly due to the nonlinear phenomenon of frequency conversion in this method. For example, VA images are speckle-free, which is a significant the advantage over conventional pulse-echo imaging. VA also has the ability to image specular surfaces regardless of the orientation of the transducer with respect to the surface, while B-mode ultrasound imaging can only visualize a specular surface if the transducer is perpendicular to the surface.

VA may be used for a variety of imaging and characterization applications, including medical and industrial applications. In medical imaging, VA has been tested on breast, prostate, and thyroid. Vibro-acoustography has been used for imaging mass lesions in excised human liver, arteries, bone, and microbubbles.

Although VA is primarily an imaging technique, methods for quantitative estimation of viscoelastic parameters of tissue using inverse problem approaches have been presented. The authors studied several finite-element experiments and solved for the material properties using simulated vibro-acoustic data. Comparisons of vibro-acoustic experiments and finite-element inverse problem solutions have shown good agreement.

2.3 Elastography in Breast Tumor Detection

Breast ultrasounds are used mainly to further examine breast abnormalities detected by a physician during a physical exam or mammogram.

The single most important factor affecting the accuracy of ultrasounds is breast density. In a study of 3,626 women with dense breasts, ultrasounds were used instead of physical exams to detect abnormalities. This study found that the number of breast cancer cases found by ultrasound was 17% higher than those found by physical exams.

The images below show ultrasound results for a normal breast (left) and a breast containing a cyst (right)

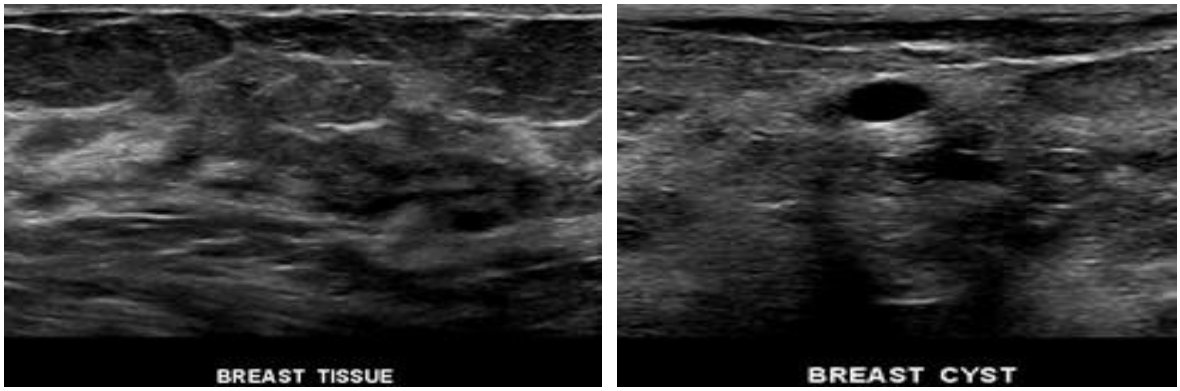

Figure2 5: Breast Cyst

*Image courtesy of Brent Burbridge, MD Saskatoon Medical Imaging, Saskatoon Canada.

Over 50% of women under the age of 50 and about 33% of women over 50 have dense breasts. Young women have breasts that are dense and full of milk glands, sometimes making mammograms difficult to interpret. For this reason, many physicians will recommend that women under the age of 30 who have a lump in their breast get an ultrasound exam before a mammogram.

Ultrasound is also used today for women with breast implants. Since there is very little tissue around a silicone implant to be x-rayed, mammograms are not always useful to detect abnormalities. Ultrasounds are also used as an alternative imaging method for pregnant women because they should not be exposed to x-rays.

2.4 Basic Medical Imaging Methods

Medical imaging can be used for both diagnosis and therapeutic purposes, making it one of our most powerful resources available to effectively care for our patients.

In terms of diagnosis, common imaging types include:

- CT (Computed Tomography)
- MRI (Magnetic Resonance Imaging)
- Ultrasound
- X-ray

They each work slightly differently to create images of what's going on inside the body, so let's look at them a little closer.

2.4.1 Ultrasound Imaging

Ultrasound is the safest form of medical imaging and has a wide range of applications. There are no harmful effects when using **ultrasound and it's one of the most cost-effective forms of medical imaging** available to us, regardless of our specialty or circumstances.

Ultrasound uses sound waves rather than ionizing radiation. High-frequency sound waves are transmitted from the probe to the body via the conducting gel, those waves then bounce back when they hit the different structures within the body and that is used to create an image for diagnosis.

Figure2 6: Ultrasound Probe

Another type of ultrasound commonly used is the 'Doppler' – a slightly different technique of using sound waves that allows the blood flow through arteries and veins to be seen.

Due to the minimal risk of using Ultrasound, it's the first choice for pregnancy, but as the applications are so wide – emergency diagnosis, cardiac, spine and internal organs – it tends to be one of the first ports of call for many patients.

2.4.2 X-Ray Imaging

X-ray imaging – the oldest but one of the most frequently used imaging types. We all know and have probably had at least one X-ray over the course of our lives.

Discovered back in 1895, X-rays are a form of electromagnetic radiation.

X-rays work on a wavelength and frequency that we're unable to see with the naked, human eye, but can penetrate through the skin to create a picture of what's going on beneath.

Typically used for diagnosing issues with the skeletal system, X-rays can also be used to detect cancer through mammography and digestive issues through barium swallows and enemas.

Figure2. 7: Setup of Ultrasound application

X-rays are widely used as they are low cost, quick and relatively easy for the patient to endure. However, there are risks associated with the use of radiation for X-ray imaging.

Every time a patient has an X-ray they receive a dose of radiation. This can go on to cause radiation-induced cancer or cataracts later in life or cause a disturbance in the growth of an embryo or fetus in a pregnant patient.

Most of these risks are mitigated by only using X-rays when strictly necessary, and correct shielding of the body.

2.4.3 Computer Tomography (CT)

CT or 'CAT' scans are a form of X-ray that creates a 3D picture for diagnosis.

Computer tomography (CT) or computed axial tomography (CAT) uses X-rays to produce cross-sectional images of the body. The CT scanner has a large circular opening for the patient to lie on a motorized table. The X-ray source and a detector then rotate around the patient producing a narrow 'fan-shaped' beam of X-rays that pass through a section of the patient's body to create a snapshot.

Figure2. 8: CT Scan machine setup

These snapshots are then collated into one, or multiple images of the internal organs and issues.

CT scans provide greater clarity than conventional X-rays with more detailed images of the internal organs, bones, soft tissue and blood vessels within the body.

The benefits of using CT scans far exceed the risks which, like with X-rays, include the risk of cancer, harm to an unborn child or reaction to a contrast agent or dye that may be used. In many cases, the use of a CT scan prevents the need for exploratory surgery.

It is crucial that when scanning children, the radiation dose has been lowered than that used for adults to prevent an unreasonable dose of radiation for the necessary imaging to be obtained. In many hospitals, you'll find a pediatric CT scanner for that reason.

2.4.3 Magnetic Resonance Imaging (MRI)

MRI scans create diagnostic images without using harmful radiation

Magnetic Resonance Imaging (MRI) uses a strong magnetic field and radio waves to generate images of the body that can't be seen well using X-rays or CT scans, i.e. it enables the view inside a joint or ligament to be seen, rather than just the outside.

Commonly used to examine internal body structures to diagnose strokes, tumors, spinal cord injuries, aneurysms, and brain function.

Figure2. 9: MRI machine setup

As we know, the human body is made mostly of water, and each water molecule contains a hydrogen nucleus (proton) which becomes aligned in a magnetic field. An MRI scanner uses a strong magnetic field to align the proton 'spins', a radio frequency is then applied which causes the protons to 'flip' their spins before returning to their original alignment.

Protons in the different body tissues return to their normal spins at different rates so the MRI can distinguish between various types of tissue and identify any abnormalities. How the molecules 'flip' and return to their normal spin alignment are recorded and processed into an image.

MRI doesn't use ionizing radiation and is increasingly being used during pregnancy with no side effects on the unborn child reported. However, there are risks associated with the use of MRI scanning and it isn't recommended as a first stage diagnosis.

As strong magnets are used, any kind of metal implant, artificial joint, etc., can cause a hazard – they can be moved or heated up within the magnetic field. There have been several reported cases where patients with pacemakers have died through the use of MRI. The loud noise from the scanner also necessitates the need for ear protection.

One thing we do have to be aware of as medical professionals in a time of escalating medical costs and increasing demand is that we're using the best resources available to meet the needs of our patients. That means a careful decision on the right medical imaging to be used for the patient and their potential diagnosis.

2.5 Advantage of Using Ultrasound

- **No exposure to radiation:** As the frequency range of the ultrasound is lower than the visible light and x-ray it does not have any radiation exposure. It is basically a sound wave frequency upper than 20,000 Hz. Frequencies used for medical diagnostic ultrasound scans extend to **10 MHz** and beyond. As the frequency is low that means it is a weak signal and it has no radiation exposure problem like an x-ray.
- **No need of injecting anything into the body:** As BUS mammography is a noninvasive process where ultrasound wave propagates through the body tissue and reflected back

which gives the image of the inner organ of our body. Here no needle is needed so it is very easy and not painful

- **No need of cutting a sample of tumor:** In case of Biopsy it is needed to cut some portion of the tumor to analyze it whether it is benign or malignant. But here in BUS technique, there is no need of doing surgery and cutting the portion of the tumor. So, BUS technique is easy, fearless and painless.
- **No risk of an increased chance of cancer:** Sometimes while doing a biopsy the benign tumor can turn into a malignant tumor because of some sort of infection and other things. But in the case of BUS technique as there is no chance of spreading of infection (as it is noninvasive), no risk of an increased chance of cancer.
- **Very cheap and economical:** BUS technique is very much cheap. In every hospital and clinic have the Ultrasound imaging facility. Moreover, nowadays in a smartphone it is implemented.
- **No side effect on human tissue:** BUS technique has no side effect on human tissue. It is very easy and harmless process.

Chapter 3

Methodology

We have taken 2 different approaches to select the best frames. The pre-processing parts for both processes are same. The algorithm that we followed is given on the next page :

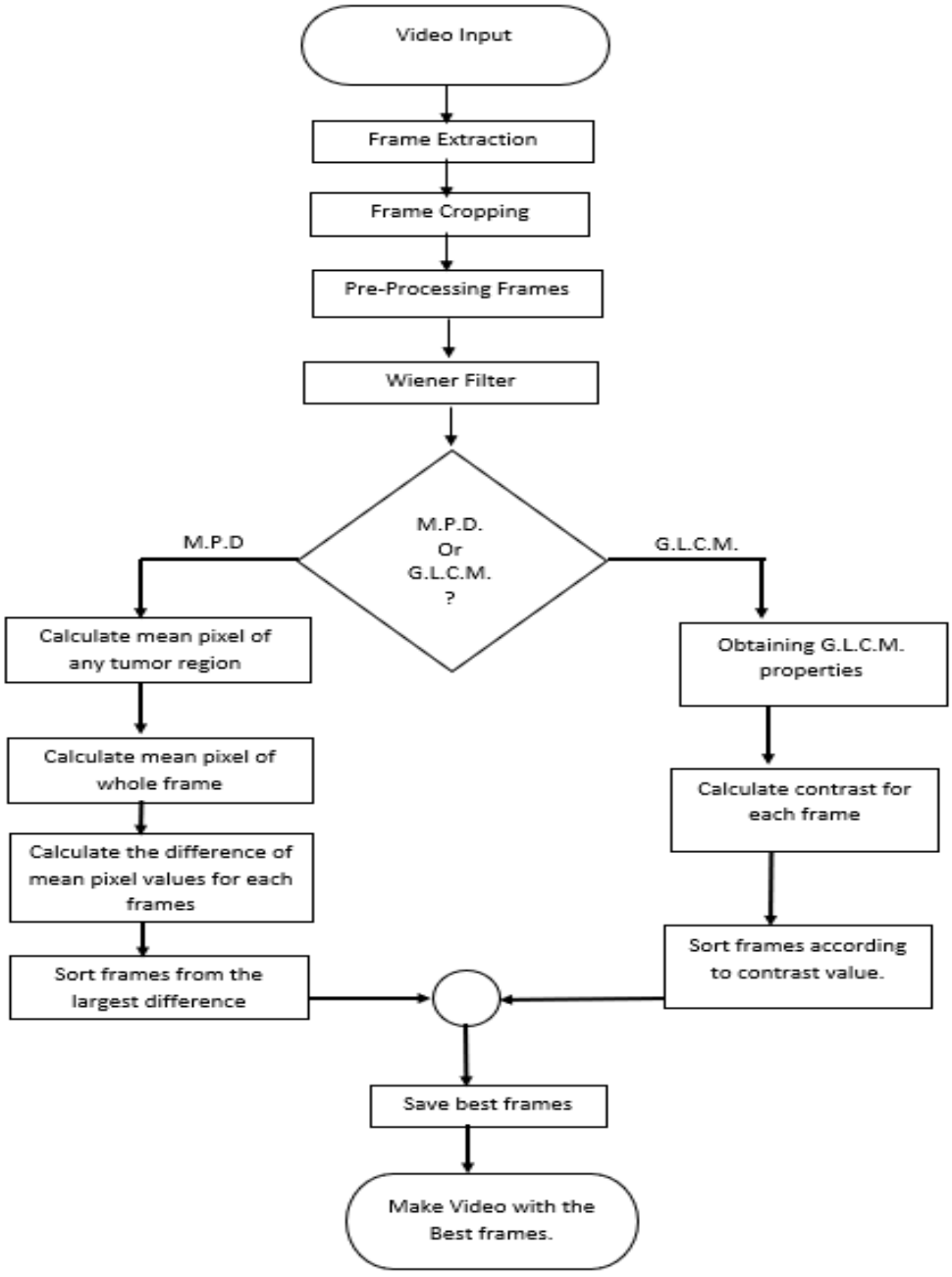

Figure3. 1: Algorithm of the method

According to our proposal, the steps are given below:

(1) Extracting frames from the video

(2) Pre-processing Frames

(3) Applying MPD & GLCM

(4) Creating a video with the best frames

3.1 Extracting frames from the video:

As the strain video is comprised of several frames, first we have to extract them. The extracted frames should then be stored and later be used for processing. Each frame is pre-processed and then their image descriptors are found.

3.2 Pre-processing Frames:

We know that ultrasound doesn't give high quality/resolution images. The frames are noisy and there are a lot of speckles. The first task is to reduce the noise and smoothing the frame without degrading the necessary information.

One of the most challenging tasks in ultrasound image processing is pre-processing. As the variety of noise cannot be pre-determined and different frames introduce a different type of distortion, it is very difficult to select a common way of smoothing all the frames. After numerous trial and error, we found that the Wiener filter is pretty good to pre-process the frames. the Wiener filter is a filter used to produce an estimate of a desired or target random process by linear time-invariant (LTI) filtering of an observed noisy process, assuming known stationary signal and noise spectra, and additive noise. The Wiener filter minimizes the mean square error between the estimated random process and the desired process.

In this filter, we are using both the Gaussian and the Median filter. The gaussian filter is a filter whose impulse response is a Gaussian function (or an approximation to it). Gaussian filters have the properties of having no overshoot to a step function input while minimizing the rise and fall time. The median filter is a nonlinear digital filtering technique, often used to remove noise from an image or signal. Such noise reduction is a typical pre-processing step to improve the results of later processing. We applied the filter 7 times on a single frame to increase the smoothing effect. After filtering, speckle reduces significantly and tumor visibility increases.

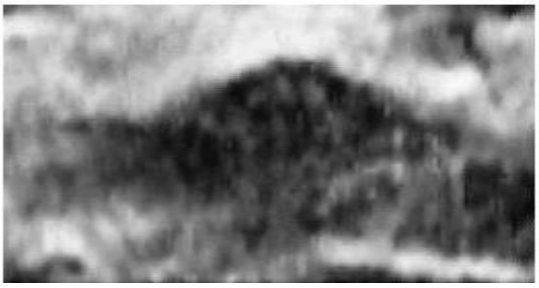

Before Pre-processing

After Pre-processing

Figure3. 2: US Image of Pre & Post processing image

3.3 Applying MPD & GLCM:

To find out the information regarding the tumor visibility thus the best frames, we have applied two different ways. They are –

1- Mean pixel Difference (MPD) method

2- Grey Level Co-occurrence matrix

3.3.1 MPD method:

From the characteristics of BUS images, we know that the tumor area has fewer pixel values than the surrounding tissue. Thus, the tumor looks darker than the background.

So, if we can select a region of interest with the tumor area as the center and take the average of the pixel value of that are, it will be comparatively lower than the average pixel value of the whole frame. Now, if in any frame, the tumor is noisy, meaning there are speckles in the frame, the mean pixel value is higher because of the white noise pixels inside the dark tumor area which have higher pixel values. So, the difference between the mean pixel value of the tumor and that of the whole frame is lower for the noisy frame. Again, frames with high tumor visibility have fewer speckles in the tumor area. That means the white noise pixels are much less in these cases. This results in a higher difference between the mean pixel value of the tumor and that of the whole frame.

If we take the mean pixel difference as a key feature to distinguish between the frames, we can easily sort out the frames according to their visibility. Frames with a higher difference have better visibility and frames with a lower difference have lower visibility.

According to the described method, we manually select a region of interest in a frame. A vague idea about the location of the tumor can be obtained by going through the strain video once. On the basis of that, the tumor region can be selected. This region remains constant for all the frames. Then the mean pixel value of the selected region and the whole frame is calculated. The mathematical mean of the pixel values within both the whole frame and the selected tumor region can be found using the following equation:

$$Pixel_{average} = \frac{\sum_{i=1}^{N} i^{th}\ pixel\ value}{N}$$

Where N = Number of pixels within the area

Then, we find out the difference between these. In this way, the mean pixel differences of all the frames are calculated and stored. Finally, we sort the frames according to MPD values.

Due to human error, it might happen that the tumor doesn't stay at the same point while taking the ultrasonography. It might move in a certain direction. In order to overcome this shortcoming, after selecting the inner tumor region, we move the selected area towards up, down, right, left, upper right, upper left, down right, down left and the minimum pixel average is taken as the tumor region mean pixel value, because of tumor region having relatively lower pixel values.

3.3.2 GLCM:

The other way to find the required frames is to calculate the Grey Level Co-occurrence Matrix (GLCM) properties for each frame as the image descriptor. GLCM is a texture character profile and this profile mention to touch i.e. smooth, silky, rough and so on. Among all of the features of GLCM, the property of 'contrast' was used. In short form, it is called a CON. 'Sum of Square Variance' is another name of Contrast. It defers the calculation of the intensity contrast linking pixel and its neighbor over the whole image. At constant image contrast value is 0. In contrast measure, weight increases exponentially (0,1,4,9) as persists from the diagonal.

$$\sum_{i,j} p(i,j)|i-j|^2$$

Contrast is the difference in luminance or color that makes an object (or its representation in an image or display) distinguishable. In visual perception of the real world, contrast is determined by the difference in the color and brightness of the object and other objects within the same field of view [17]. GLCM.Contrast returns a measure of the intensity contrast between a pixel and its neighbor over the whole image. It is low if the tumor is visible and is uniform. If there is noise, making the tumor not visible, there is no uniformly distributed tumor region and the GLCM. Contrast value is relatively high. So, if the tumor is more visible in any frame, in other words, distinguishable from the surrounding tissue, it will have lower GLCM.Contrast value than the not visible ones.

Following this process, we calculate the GLCM. Contrast property for each of the frames and sort them in ascending order. The corresponding frames are sorted at the same time and the required frames are found.

3.4 Creating a video with the best frames:

We merge a required number of frames to form two videos where the tumor is most visible. 10 best frames from both MPD and GLCM.Contrast methods are taken to form the videos. The doctor/radiologist may use these two videos to identify the tumor easily. There is no need of going through all the frames manually and sorting them out.

Chapter 4

Result and Calculation

4.1 Calculations:

We've applied the process on 9 videos. Their error calculation is given in the table below:

VIDEO INPUT	BEST FRAMES No. (MANUAL)	MPD	GLCM (CONTRAST)	ACCURACY OF MPD (PERCENTAGE)	ACCURACY OF GLCM (PERCENTAGE)
1	43, 213, 248, 266, 156, 84, 100, 105, 271, 45	43, 213, 248, 266, 145, 84, 100, 112, 271, 45	43, 213, 248, 266, 145, 90, 100, 117, 271, 55	80%	70%
2	146, 124, 115, 120, 122, 202, 205, 75, 165, 212	146, 124, 115, 120, 129, 202, 245, 75, 165, 220	155, 124, 85, 120, 131, 202, 205, 75, 165, 221	70%	60%
3	228, 174, 171, 175, 235, 92, 122, 165, 168, 172	228, 174, 171, 175, 235, 92, 122, 165, 200, 179	228, 174, 171, 183, 235, 55, 130, 165, 168, 181	80%	60%
4	26, 269, 309, 312, 271, 77, 223, 228, 155, 161	26, 269, 309, 312, 271, 85, 223, 228, 155, 161	26, 285, 309, 322, 271, 77, 223, 228, 175, 161	90%	70%
5	79, 211, 102, 106, 108, 226, 56, 128,245, 250	79, 211, 117, 106, 108, 288, 56, 128,245, 265	79, 236, 102, 106, 117, 226, 68, 128,245, 268	70%	60%

Table 4.1: error calculation of 9 videos

Now the results of the videos are given serially:

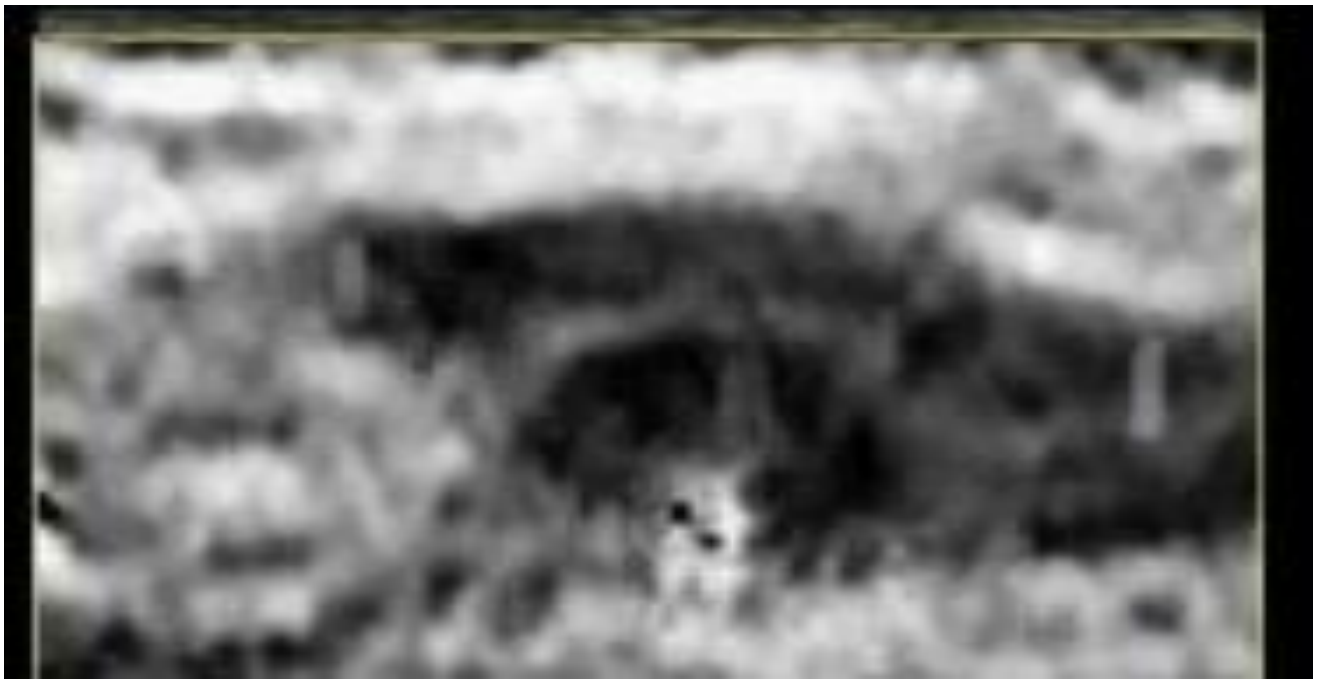

(a1)

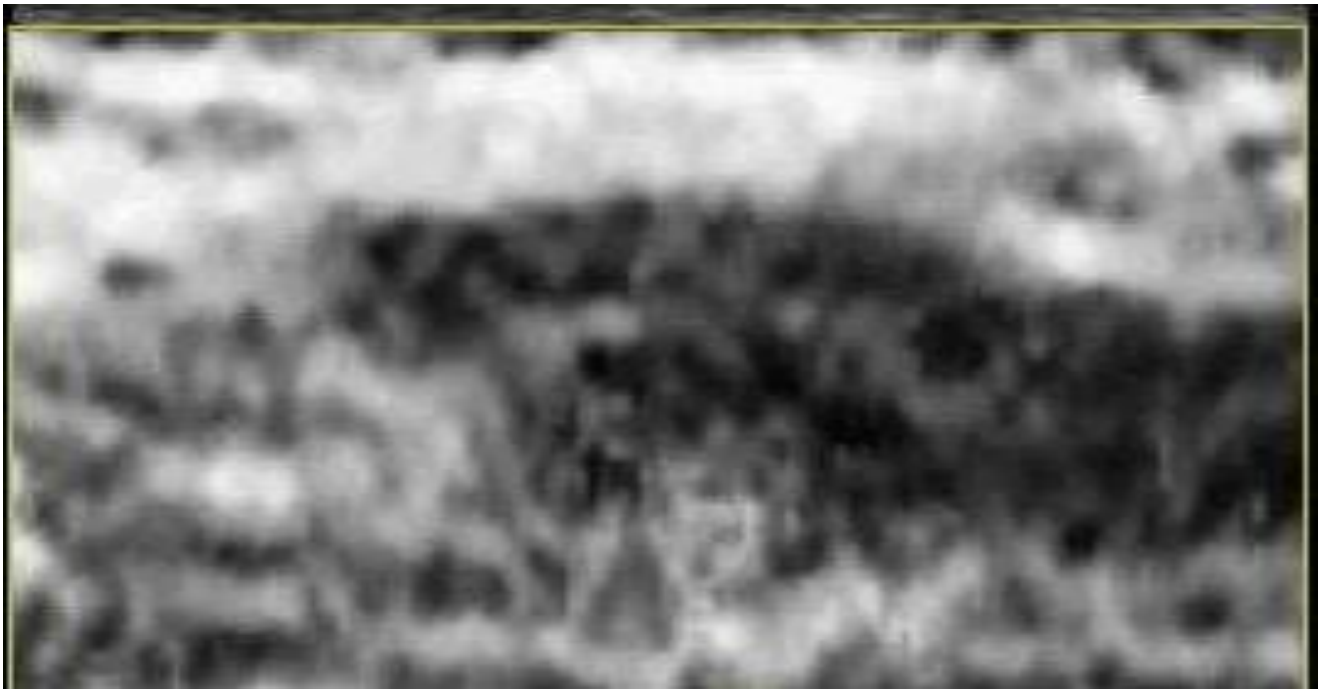

(b1)

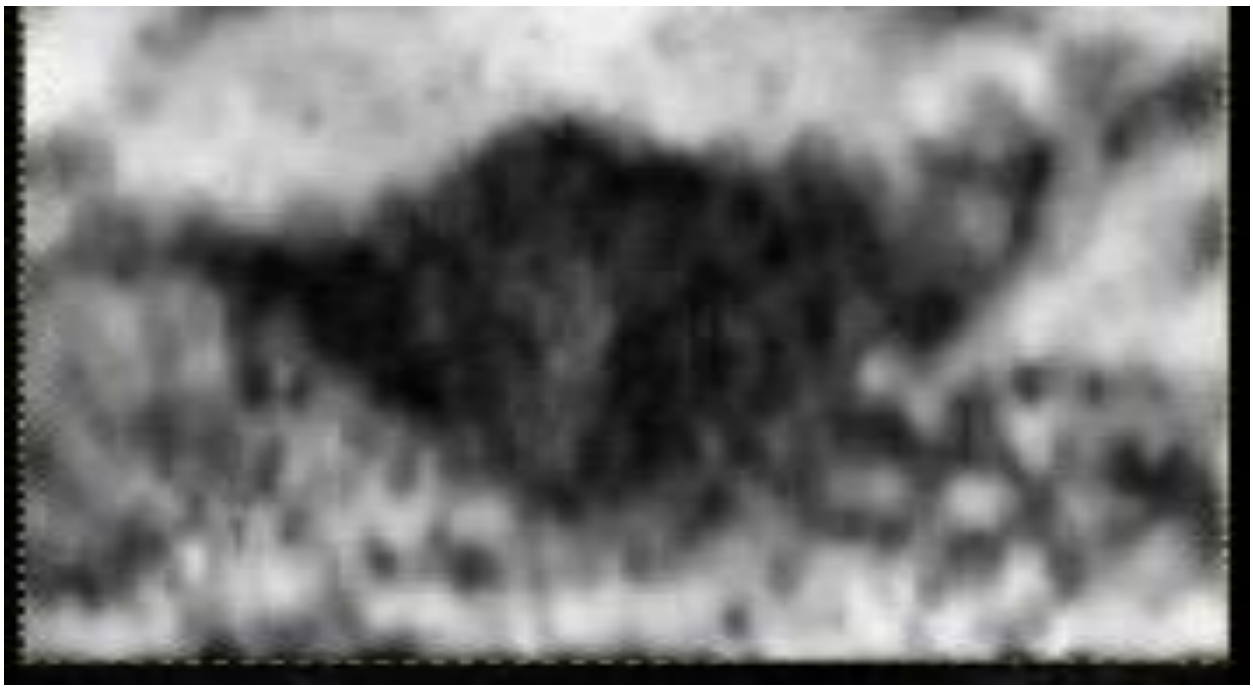

(a2)

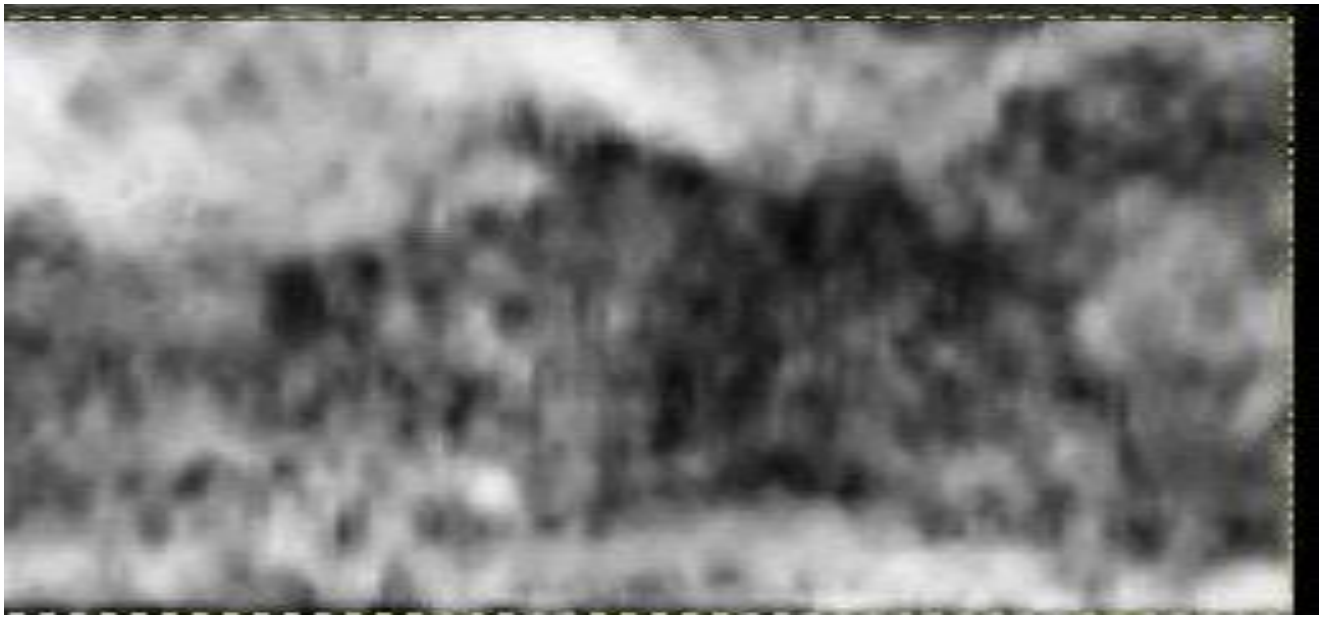

(b2)

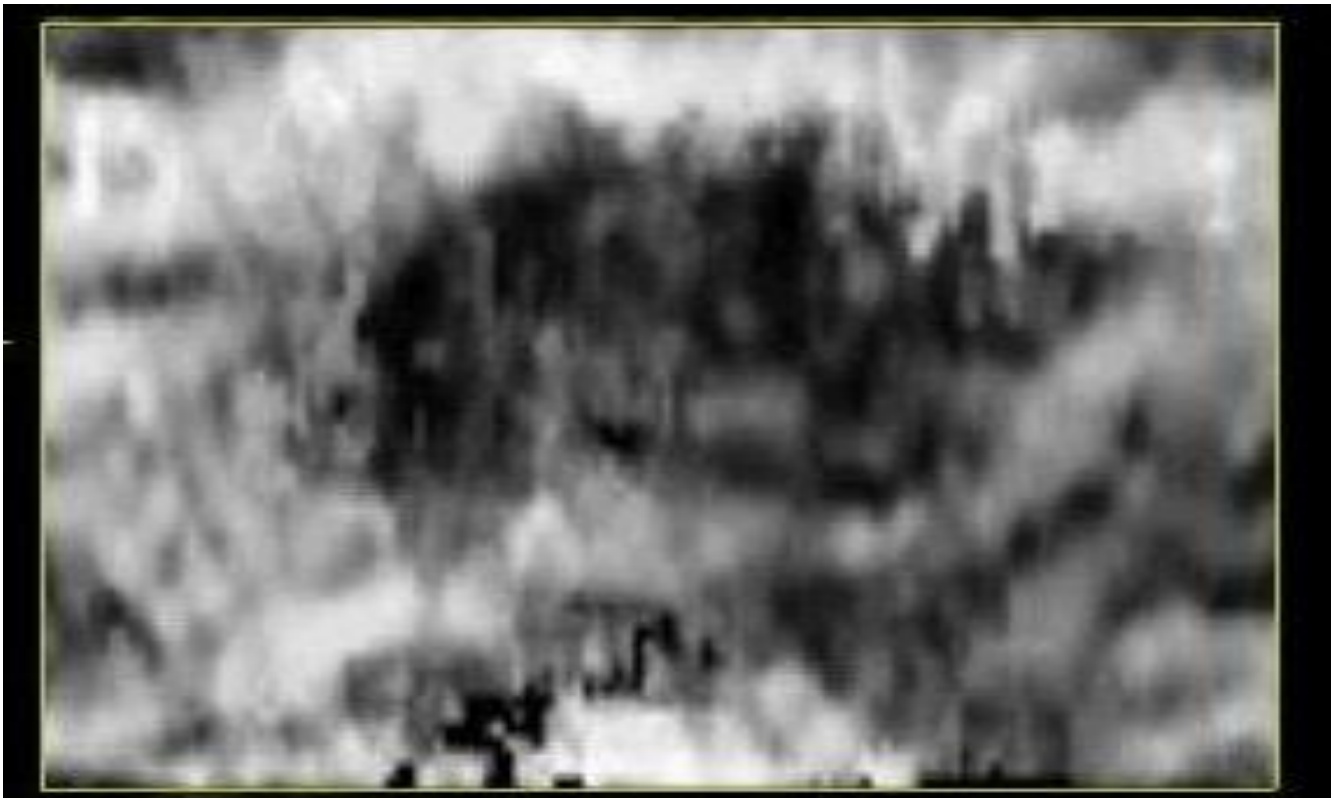

(a3)

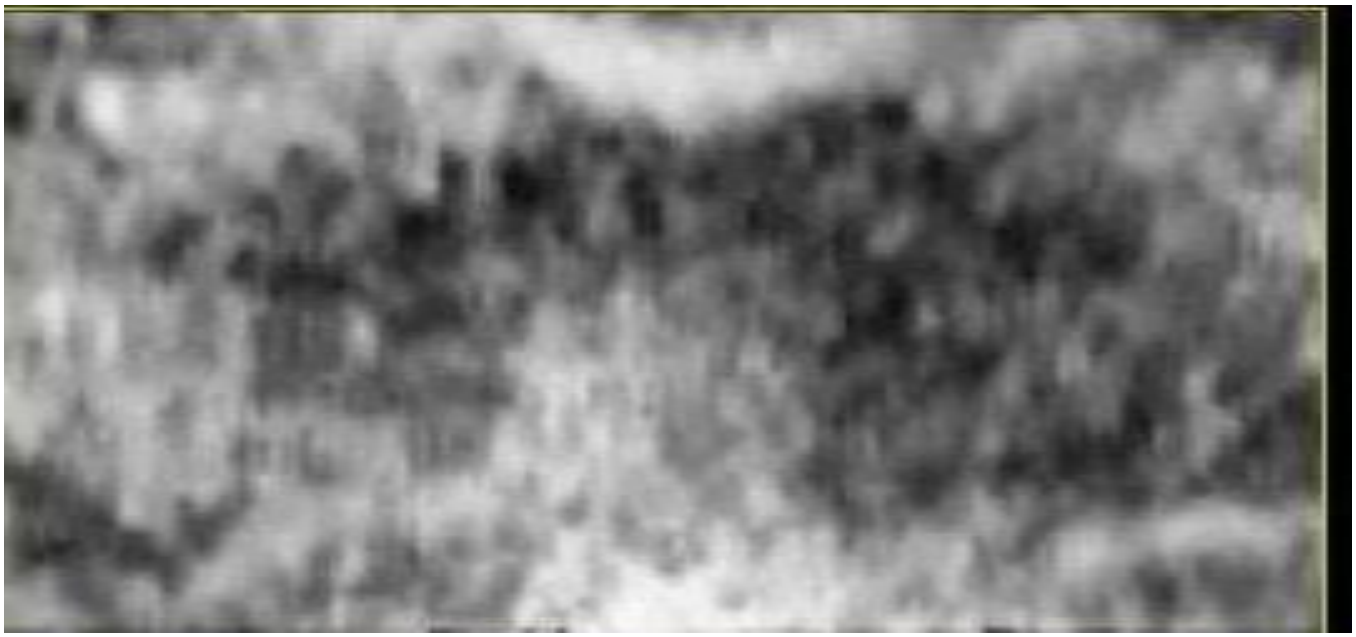

(b3)

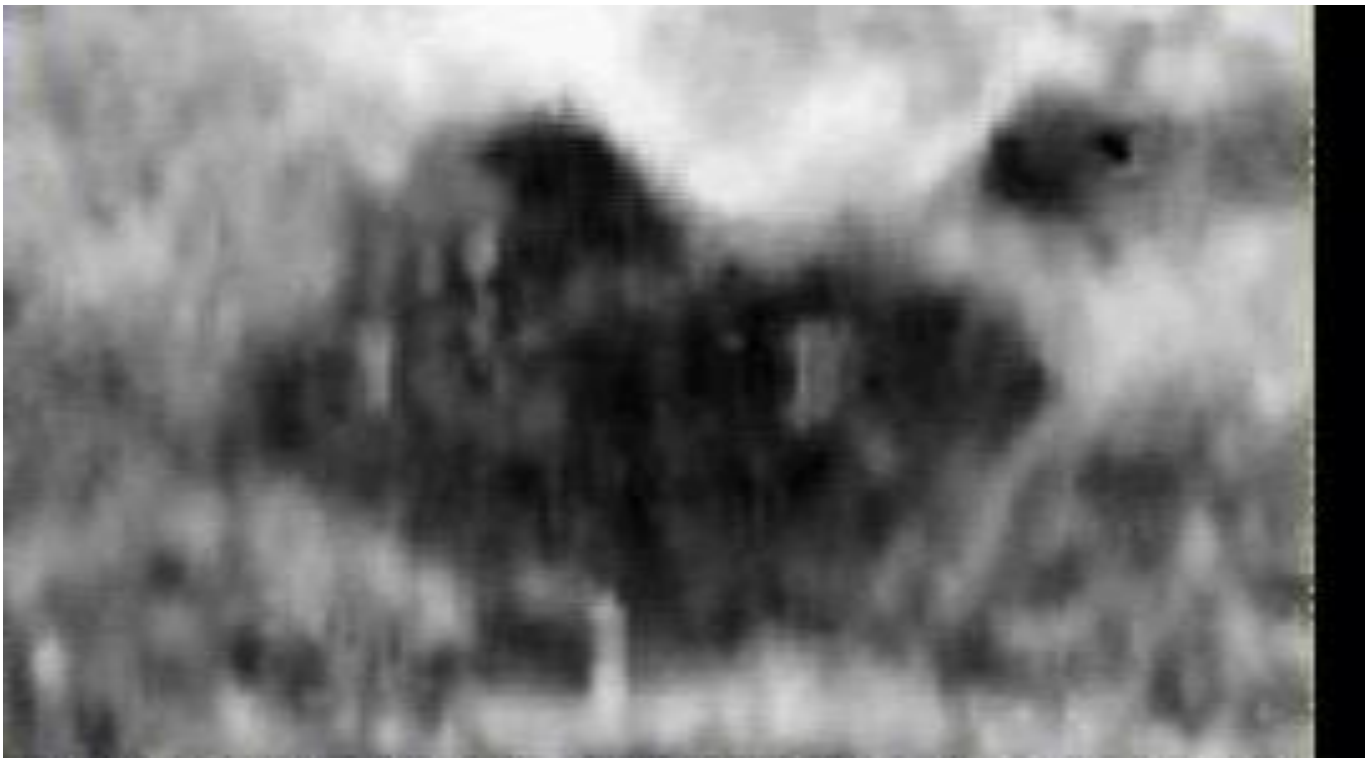

(a4)

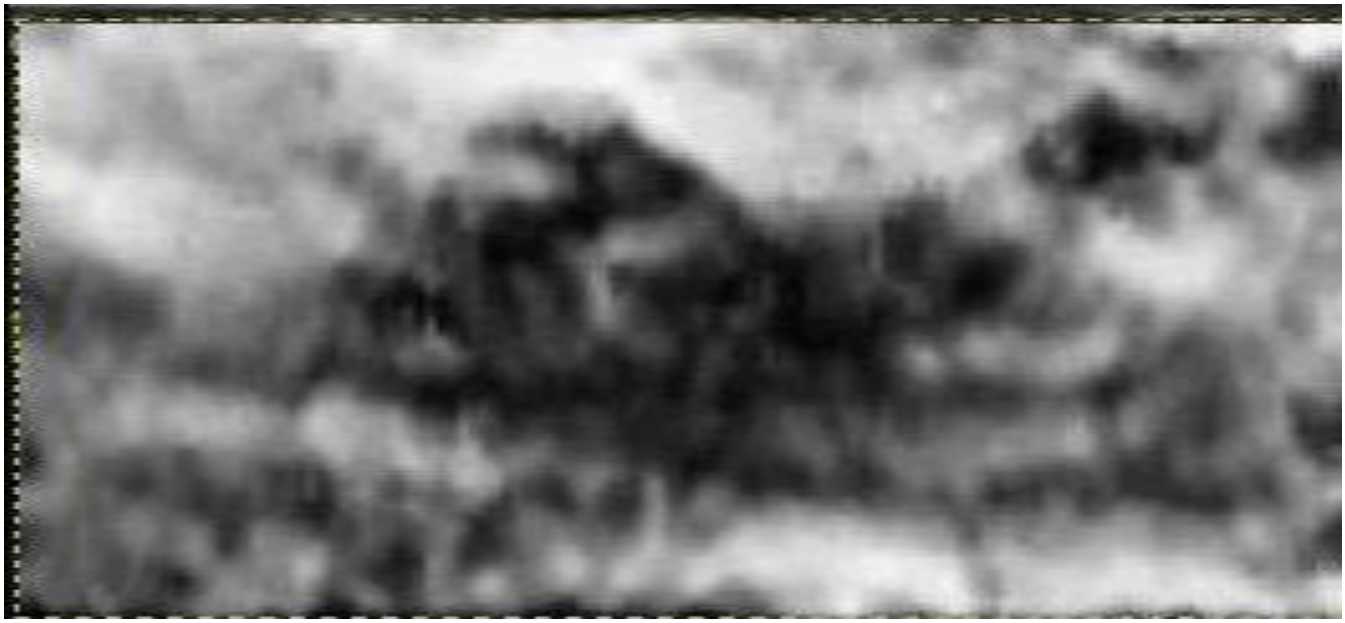

(b4)

(a5)

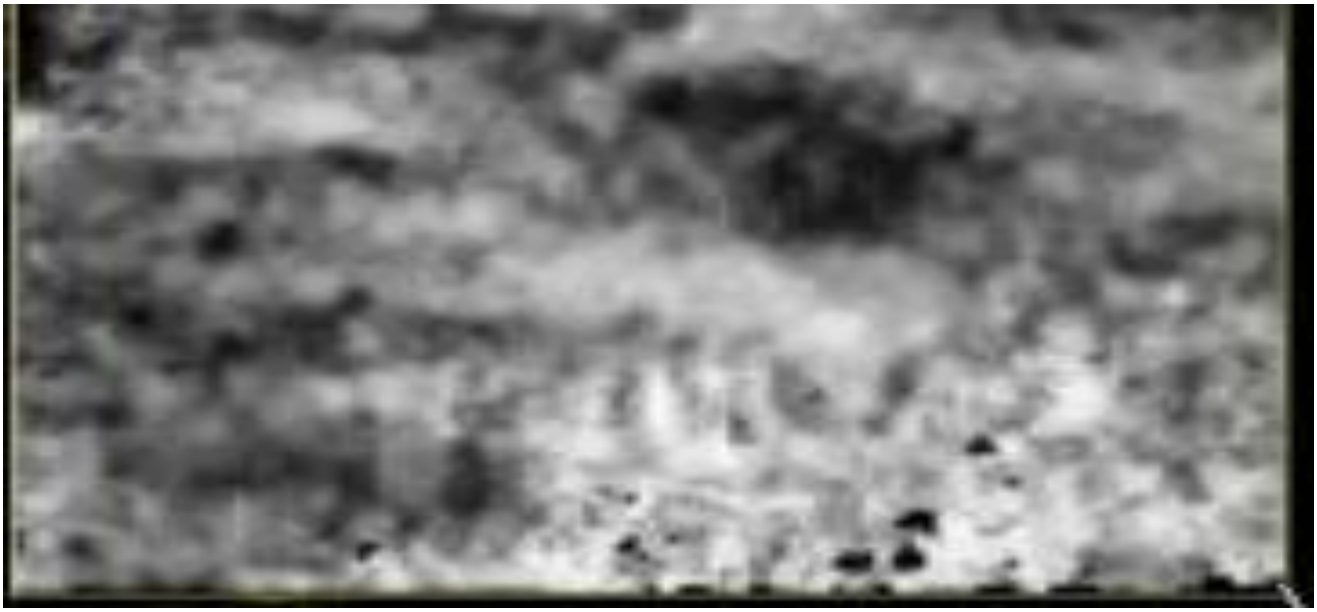

(b5)

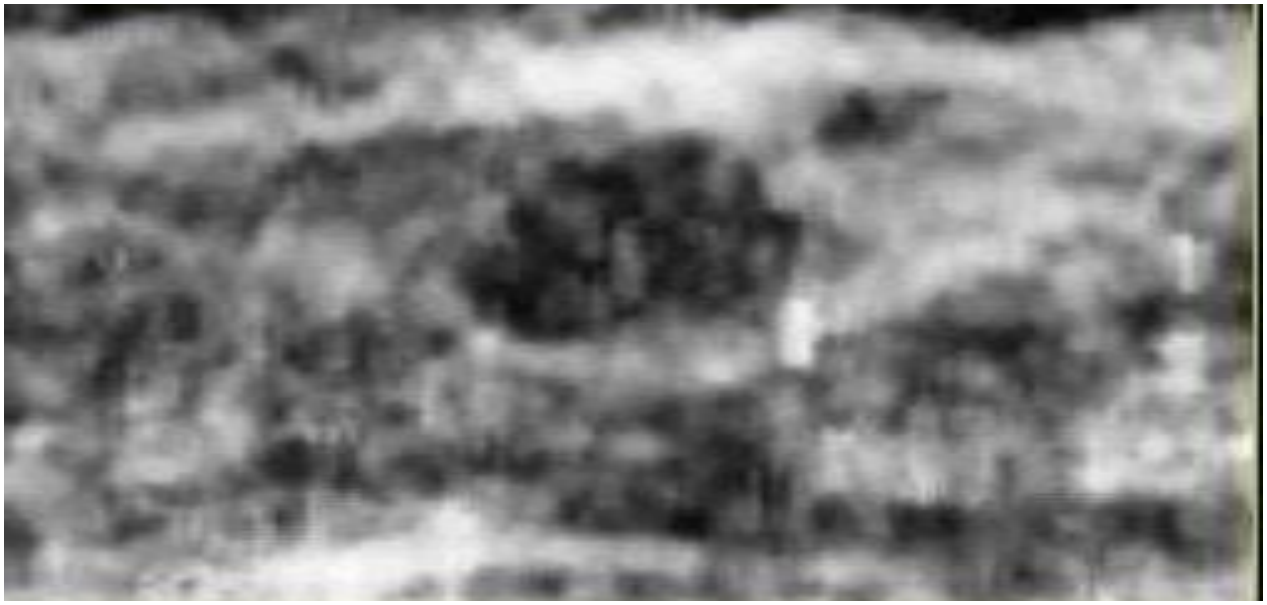

(а6)

(b6)

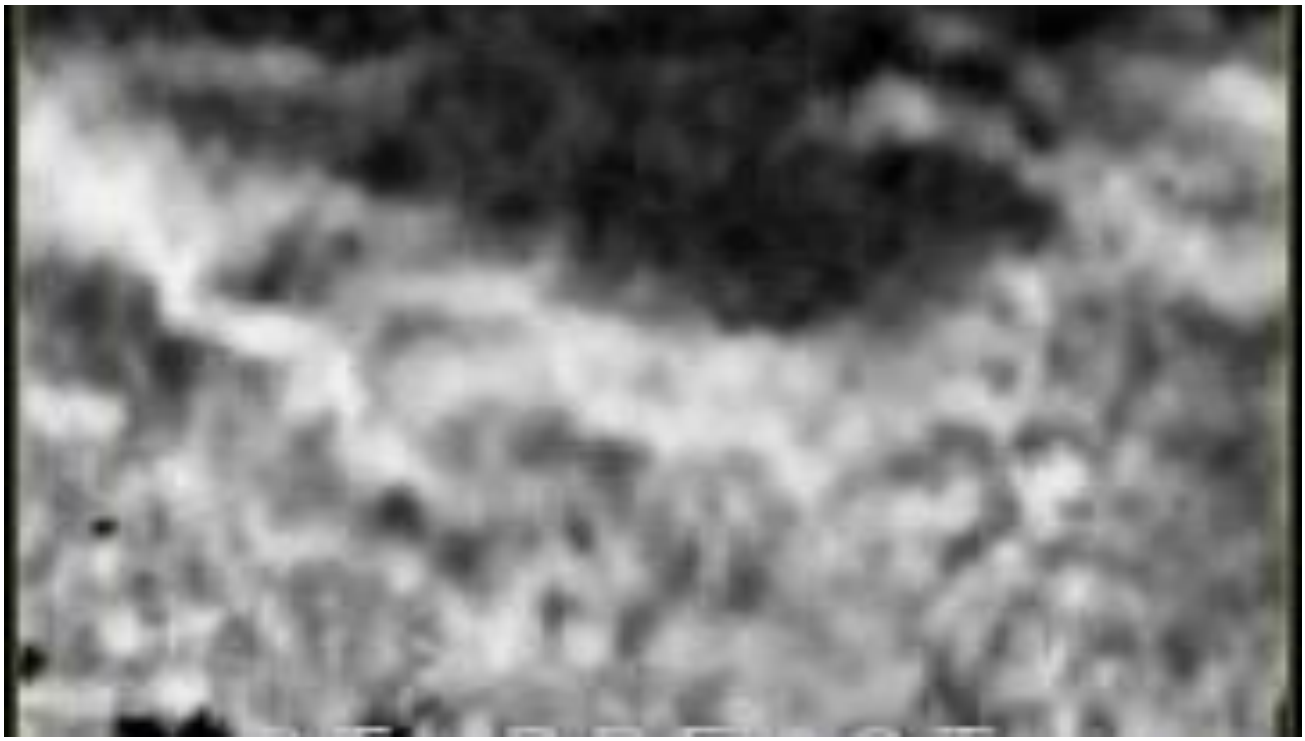

(a7)

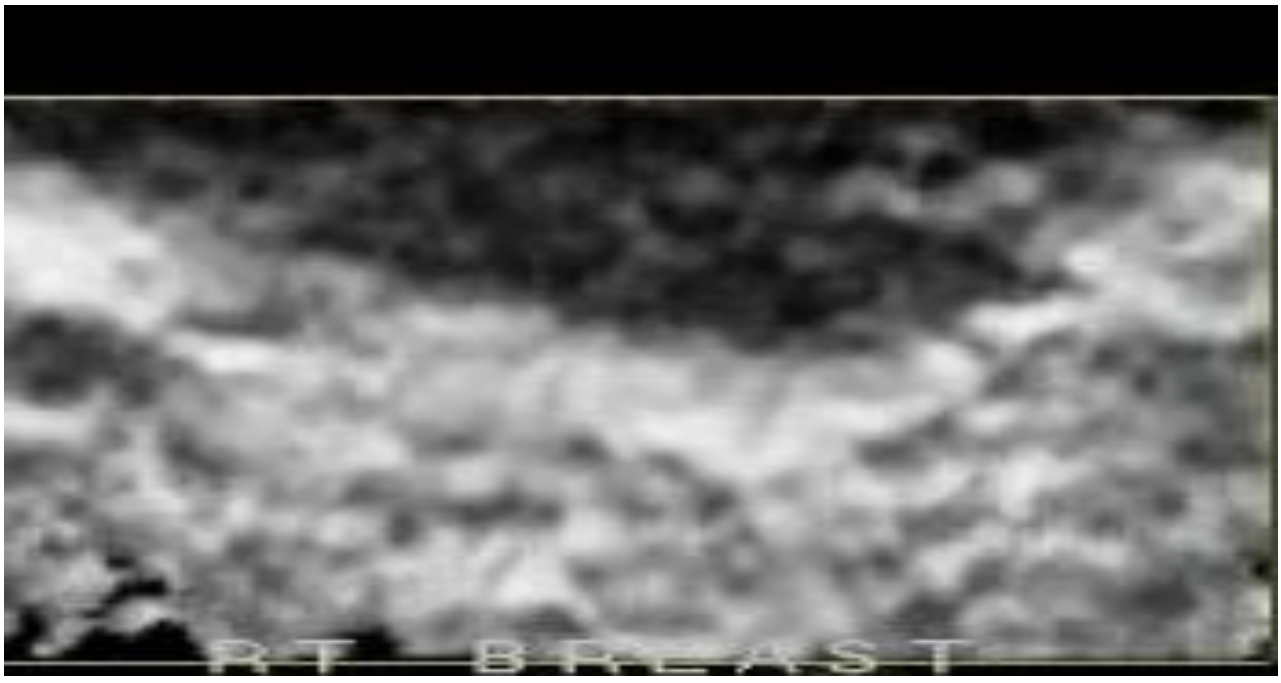

(b7)

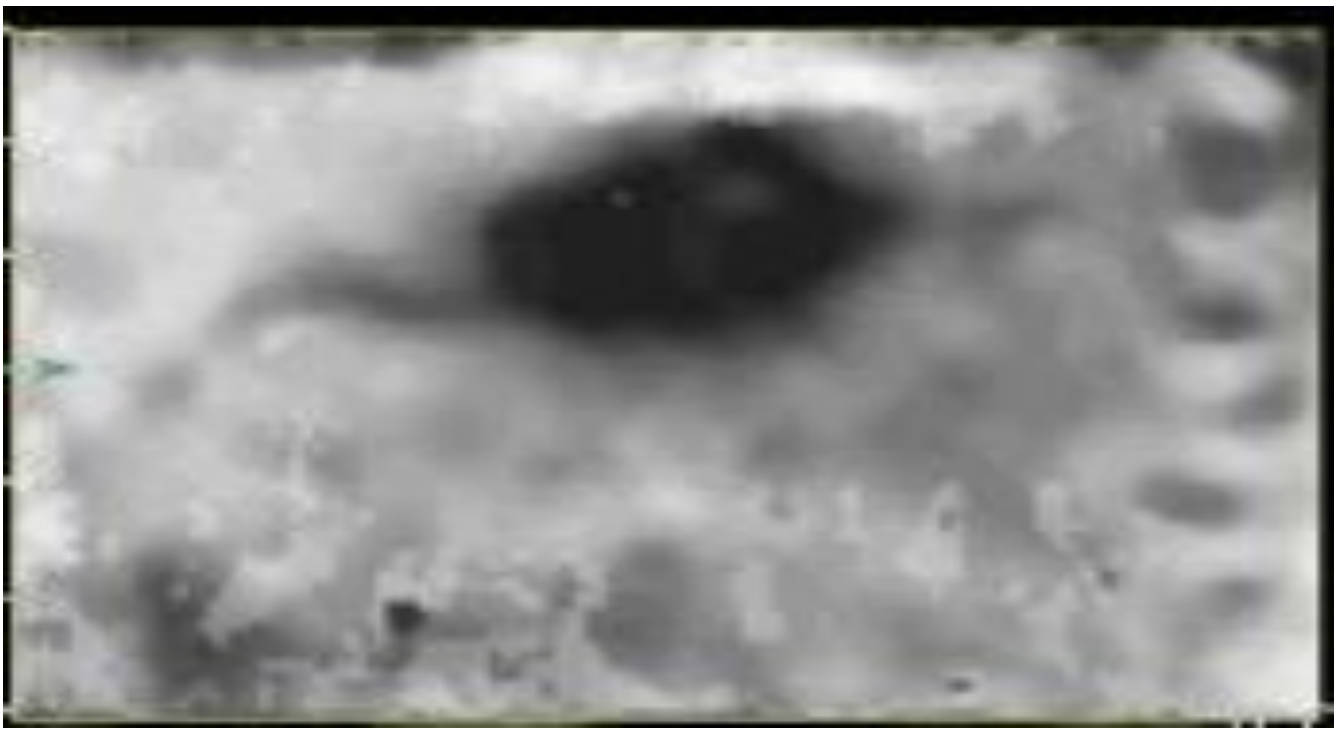

(a8)

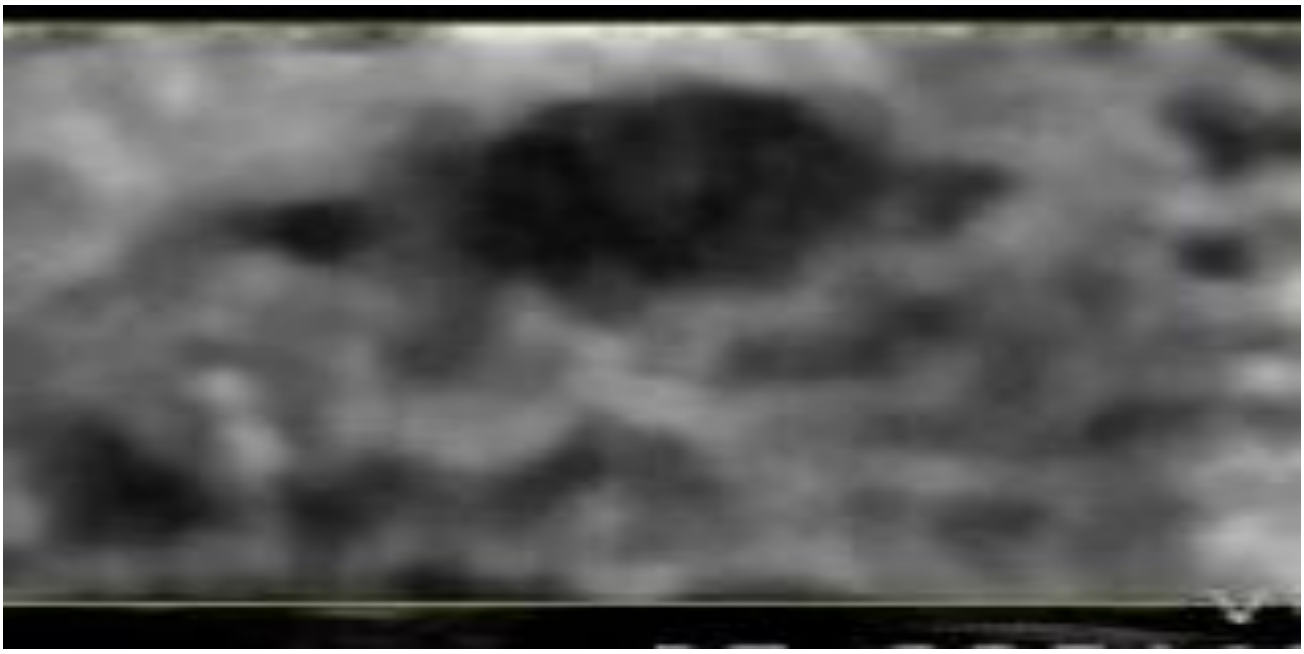

(b8)

(a9)

(b9)

Figure4. 1: (a)Results from MPD (Mean Pixel Difference)

(b)Result from GLCM

Chapter 5

Discussion

5.1 Demerits of Ultrasound

In spite of possessing a lot of good sides of Ultrasound; it also has some bad sides as well. Those are: [49]

- Ultrasound results may identify a potential area of concern that is not malignant. These false-positive results could lead to more procedures, including biopsies, that are not necessary 8. Preliminary data from a trial being conducted showed that there was a higher rate of false-positive results with ultrasounds than with mammography (2.4%-12.9% for ultrasound and 0.7%-6% for mammography).
- Although ultrasound is often used in an attempt to prevent an invasive measure for diagnosis, sometimes it is unable to determine whether or not a mass is malignant, and a biopsy will be recommended.
- Many cancers cannot be detected via an ultrasound.
- Calcifications that are visible on mammograms are not visible on ultrasound scans, thereby preventing early diagnosis of the portion of breast cancers that begin with calcifications.
- Ultrasounds are not available everywhere, and not all insurance plans cover them.8
- An ultrasound requires a highly experienced and skilled operator to detect a malignant lump, as well as good equipment. If the cancerous tissue is not detected at the time of the scan, it will not be caught as early as possible. The ACR-accredited facilities database is a good way to determine the expertise of a facility in ultrasound imaging.

Due to this, it is one of the toughest signals to deal with in terms of image processing. That's why a lot of the images are seen very bad in shape. However, we are trying to proceed in future in a more efficient way to deal with it.

5.2 Future Work

The method that we've established is semi-automatic one. So, our next main priority is to make it fully automatic one. For that, we are going to implement the segmentation concept so that the system can automatically distinguish the segment of the tumor and the background. Then depending on the number of noises in the tumor section, it will sort the best frames. Then it will take the system one step ahead.

Then we are planning to make the system a decision making one which will be acquainted with a lot of the parameters of cancer. Then it will be trained by a lot of malignant and benign tumors data. So, after that, it will be able to differentiate a malignant tumor from a benign tumor.

So, this two furthermore approach will make a complete cancer detection software, which was our main target.

References

1. Cheng, H.D., Shan, J., Ju, W., Guo, Y., and Zhang, L. Automated breast cancer detection and classification using ultrasound images: A survey. *Pattern Recognition 43,* 1 (2010), 299-317.

2. Jemal, A., Siegel, R., Xu, J., and Ward, E. Cancer statistics 2010. *CA Cancer J. for Clininicians 60,* (2010), 227-300.

3. Cheng, H.D., Shi, X.J., Min, R., Hu, L.M., Cai, X.P., and Du, H.N. Approaches for automated detection and classification of masses in mammograms. *Pattern Recognition 39,*

4 (2006), 646-668. 4. Cheng, H.D., Cai, X., Chen, X., Hu, L., and Lou, X. Computer-aided detection and classification of microcalcifications in mammograms: A survey. *Pattern Recognition 36,* 12 (2003), 2967-2991.

5. Jesneck, J., Lo, J., and Baker, J. Breast mass lesions: Computer-aided diagnosis models with mammographic and sonographic descriptors. *Radiology 244*, 2 (2007), 390-398.

6. Shankar, P.M., Piccoli, C.W., Reid, J.M., Forsberg, F., and Goldberg, B.B. Application of the compound probability density function for characterization of breast masses in ultrasound B scans. *Physics in Medicine & Biology 50,* 10 (2005), 2241-2248.

7. Taylor, K.J.W., Merritt, C., Piccoli, C., Schmidt, R., Rouse, G., Fornage, B., Rubin, E., Georgian-Smith, D., Winsberg, F., Goldberg, B., and Mendelson, E. Ultrasound as a complement to mammography and breast examination to 86 characterize breast masses. *Ultrasound in Medicine & Biology 28*, 1 (2002), 19- 26.

8. Zhi, H., Ou, B., Luo, B.-M., Feng, X., Wen, Y.-L., and Yang, H.-Y. Comparison of ultrasound elastography, mammography, and sonography in the diagnosis of solid breast lesions. *J. Ultrasound in Medicine 26*, 6 (2007), 807-815.

9. Chang, R.-F., Wu, W.-J., Moon, W.K., and Chen, D.-R. Improvement in breast tumor discrimination by support vector machines and speckle-emphasis texture analysis. *Ultrasound in Medicine & Biology 29,* 5 (2003), 679-686.

10. Sahiner, B., Chan, H.-P., Roubidoux, M.A., Hadjiiski, L.M., Helvie, M.A., Paramagul, C., Bailey, J., Nees, A.V., and Blane, C. Malignant and benign breast masses on 3D US volumetric images: Effect of computer-aided diagnosis on radiologist accuracy. *Radiology 242*, 3 (2007), 716-724.

11. Chen, C.-M., Chou, Y.-H., Han, K.-C., Hung, G.-S., Tiu, C.-M., Chiou, H.-J., and Chiou, S.-Y. Breast lesions on sonograms: Computer-aided diagnosis with nearly setting-independent features and artificial neural networks. *Radiology 226*, 2 (2003), 504-514.

12. Drukker, K., Giger, M.L., Horsch, K., Kupinski, M.A., Vyborny, C.J., and Mendelson, E.B. Computerized lesion detection on breast ultrasound. *Medical Physics 29*, 7 (2002), 1438-1446.

13. Andr, M.P., Galperin, M., Olson, L.K., Richman, K., Payrovi, S., and Phan, P. Improving the accuracy of diagnostic breast ultrasound. *Acoustical Imaging 26*, (2002), 453-460. 87

14. Huang, Y.-L., Chen,D.-R., and Liu, Y.-K. Breast cancer diagnosis using image retrieval for different ultrasonic systems. In *International Conference on Image Processing*, 2004, 2957-2960.

15. Anderson, B., Shyyan, R., Eniu, A., Smith, R., and Yip, C. Breast cancer in limited-resource countries: An overview of the breast health global initiative 2005 guidelines. *Breast Journal 12*, 1 (2006), S3-15.

16. Hwang, K.-H., H., Lee, J.G., Kim, J.H., Lee, H.-J. Om, K.-S., Yoon, M., and Choe, W. Computer aided diagnosis (CAD) of breast mass on ultrasonography and scintimammography. In *Proceedings of 7th International Workshop on Enterprise Networking and Computing in Healthcare Industry*, 2005, 187-189.

17. American-College-of-Radiology, ACR standards 2000-2001. 2000: Reston, VA.

18. Noble, J.A. and Boukerroui, D. Ultrasound image segmentation: A survey. *IEEE Trans. on Medical Imaging 25*, 8 (2006), 987-1010.

19. Joo, S., Moon, W.K., and Kim, H.C. Computer-aided diagnosis of solid breast nodules on ultrasound with digital image processing and artificial neural network. In *26th Annual IEEE International Conference Proceedings on Engineering in Medicine and Biology Society*, 2004, 1397-13400.

20. Chen, D.-R., Chang, R.-F., and Huang, Y.-L. Computer-aided diagnosis applied to US of solid breast nodules by using neural networks. *Radiology 213*, 2 (1999), 407-412. 88

21. Madabhushi, A. and Metaxas, D.N. Combining low-, high-level and empirical domain knowledge for automated segmentation of ultrasonic breast lesions. *IEEE Trans. on Medical Imaging 22*, 2 (2003), 155-169.

22. Xiaohui, H., Bruce, C.J., Pislaru, C., and Greenleaf, J.F. Segmenting highfrequency intracardiac ultrasound images of myocardium into infarcted, ischemic, and normal regions. *IEEE Trans. on Medical Imaging 20*, 12 (2001), 1373-1383.

23. Joo, S., Yang, Y.S., Moon, W.K., and Kim, H.C. Computer-aided diagnosis of solid breast nodules: Use of an artificial neural network based on multiple sonographic features. *IEEE Trans. on Medical Imaging 23*, 10 (2004), 1292- 1300.

24. Yeh, C.-K., Chen, Y.-S., Fan, W.-C., and Liao, Y.-Y. A disk expansion segmentation method for ultrasonic breast lesions. *Pattern Recognition 42*, 5 (2009), 596-606.

25. Horsch, K., Giger, M.L., Venta, L.A., and Vyborny, C.J. Computerized diagnosis of breast lesions on ultrasound. *Medical Physics 29*, 2 (2002), 157-164.

26. Horsch, K., Giger, M.L., Venta, L.A., and Vyborny, C.J. Automatic segmentation of breast lesions on ultrasound. *Medical Physics 28*, 8 (2001), 1652-1659.

27. Chang, R.F., Wu, W.J., Moon, W.K., and Chen, D.R. Automatic ultrasound segmentation and morphology based diagnosis of solid breast tumors. *Breast Cancer Research and Treatment 89*, 2 (2005), 179-185.

28. Liu, B., Cheng, H.D., Huang, J., Tian, J., Liu, J., and Tang, X., Automated segmentation of ultrasonic breast lesions using statistical texture classification and 89 active contour based on probability distance. *Ultrasound in Medicine & Biology 35*, 8 (2009), 1309-1324.

29. Sarti, A., Corsi, C., Mazzini, E., and Lamberti, C. Maximum likelihood segmentation with Rayleigh distribution of ultrasound images. *Computers in Cardiology 31* (2004), 329-332.

30. Chang, R.-F., Wu, W.-J., Moon, W.K., Chen, W.-M., Lee, W., and Chen, D.-R. Segmentation of breast tumor in three-dimensional ultrasound images using threedimensional discrete active contour model. *Ultrasound in Medicine & Biology 29*, 11 (2003), 1571-1581.

31. Chen, D.-R., Chang, R.-F., Wu, W.-J., Moon, W.K., and Wu, W.-L. 3-D breast ultrasound segmentation using active contour model. *Ultrasound in Medicine & Biology 29*, 7 (2003), 1017-1026.

32. Chang, R.F., Wu, W.J., Tseng, C., Chen, D.R., and Moon, W.K. 3-D snake for US in margin evaluation for malignant breast tumor excision using mammotome. *IEEE Trans. on Information Technology in Biomedicine 7*, 3 (2003), 197-201.

33. Sahiner, B., Chan, H.-P., Roubidoux, M.A., Helvie, M.A., Hadjiiski, L.M., Ramachandran, A., Paramagul, C., LeCarpentier, G.L., Nees, A., and Blane, C. Computerized characterization of breast masses on three-dimensional ultrasound volumes. *Medical Physics 31*, 4 (2004), 744-754.

34. Boukerroui, D., Baskurt, A., Noble, J.A., and Basset, O. Segmentation of ultrasound images--multiresolution 2D and 3D algorithm based on global and local statistics. *Pattern Recognition Letters 24*, 4-5 (2003), 779-790. 90

35. Xiao, G., Brady, M., Noble, J.A., and Zhang, Y. Segmentation of ultrasound Bmode images with intensity inhomogeneity correction. *IEEE Trans. on Medical Imaging 21*, 1 (2002), 48-57.

36. Cheng, H.D., Hu, L.M., Tian, J.W., and Sun, L., A novel Markov random field segmentation algorithm and its application to breast ultrasound image analysis. In *6th International Conference on Computer Vision, Pattern Recognition and Image Processing*, 2005, 644-647.

37. Boukerroui, D., Basset, O., Guérin, N., and Baskurt, A. Multiresolution texture based adaptive clustering algorithm for breast lesion segmentation. *European J. Ultrasound 8*, 2 (1998), 135-144.

38. Christopher, L.A., Delp, E.J., Meyer, C.R., and Carson, P.L. 3-D Bayesian ultrasound breast image segmentation using the EM/MPM algorithm. In *Proceedings of IEEE International Symposium on Biomedical Imaging*, 2002, 86-89.

39. Kotropoulos, C. and Pitas, I. Segmentation of ultrasonic images using support vector machines. *Pattern Recogniton Letters 24*, 4-5 (2003), 715-727.

40. Zhan, Y. and Shen, D. Deformable segmentation of 3-D ultrasound prostate images using statistical texture matching method. *IEEE Trans. on Medical Imaging 25*, 3 (2006), 256-272.

41. Wu, H.-M. and Lu, H.H.-S. Iterative sliced inverse regression for segmentation of ultrasound and MR images. *Pattern Recognition 40*, 12 (2007), 3492-3502. 91

42. Dokur, Z. and Ölmez, T. Segmentation of ultrasound images by using a hybrid neural network. *Pattern Recognition Letters 23*, 14 (2002), 1825-1836.

43. Işcan, Z., Kurnaz, M.N., Dokur, Z., and Ölmez, T. Letter: Ultrasound image segmentation by using wavelet transform and self-organizing neural network. *Neural Information Processing - Letters and Reviews 10*, 8-9 (2006).

44. Huang, Y.-L. and Chen, D.-R. Watershed segmentation for breast tumor in 2-D sonography. *Ultrasound in Medicine & Biology 30*, 5 (2004), 625-632.

45. Gomez, W., Leija, L., Alvarenga, A.V., Infantosi, A.F.C., and Pereira, W.C.A. Computerized lesion segmentation of breast ultrasound based on markercontrolled watershed transformation. *Medical Physics 37*, 1 (2010), 82-95.

46. Huang, C.S., Wu, C.Y., Chu, J.S., Lin, J.H., Hsu, S.M., and Chang, K.J. Microcalcifications of non-palpable breast lesions detected by ultrasonography: correlation with mammography and histopathology. *Ultrasound in Obstetrics and Gynecology 13,* 6 (1999), 431-436.

47. Chen, C.-M., Chou, Y.-H., Chen, C.S.K., Cheng, J.-Z., Ou, Y.-F., Yeh, F.-C., and Chen, K.-W. Cell-competition algorithm: A new segmentation algorithm for multiple objects with irregular boundaries in ultrasound images. *Ultrasound in Medicine & Biology 31*, 12 (2005), 1647-1664.

48. Cheng, J.-Z., Chou, Y.-H., Huang, C.-S., Chang, Y.-C., Tiu, C.-M., Yeh, F.-C., Chen, K.-W., Tsou, C.-H., and Chen, C.-M. ACCOMP: Augmented cell competition algorithm for breast lesion demarcation in sonography. *Medical Physics 37*, 12 (2010), 6240-6252.

49.https://www.cancerquest.org/index.php/patients/detectionanddiagnosis/ultrasound?fbclid=IwAR3sAb9_0uScu2nJACb89bW_i_UePuncOHoiT0KKbvVGABVB1tBCcuHXzbY#benefits-disadvantages